GCAGS JOURNAL
A Publication of the Gulf Coast Association of Geological Societies
www.gcags.org

Regional Sequence Stratigraphy, Biostratigraphy, and Facies of the Upper Cretaceous Austin Chalk in South and Central Texas

Christine Griffith[1], James Pospichal[2], Eric de Kaenel[3], Michael Pope[1], and Arthur Donovan[1]

[1]*Texas A&M University, 3115 TAMU, College Station, Texas 77843–3115, U.S.A.*

[2]*BugWare, Inc., 1615 Village Square Blvd., Ste. 8, Tallahassee, Florida 32309, U.S.A.*

[3]*DPR (De Kaenel Paleo Research), Chemin sous la Roche 4b, Mont-sur-Rolle, 1185, Switzerland*

ABSTRACT

This regional study constructs a sequence stratigraphic framework for the Upper Cretaceous Austin Chalk in South and Central Texas, based on new nannofossil biostratigraphy, core descriptions, correlations of wireline logs, and synthesis of outcrop, core, and paleontological descriptions from literature. The study area extends along strike from the Rio Grande to Austin, and along dip from the outcrop belt to the limit of downdip well control at the Lower Cretaceous shelf edges. New biostratigraphic control enables correlations across the region and ties the stratigraphic nomenclature from the outcrop to the major producing petroleum fields on either side of the San Marcos Arch. The upper Turonian–lower Campanian Austin Chalk consists of three unconformity-bounded sequences, with a basal unconformity, two internal unconformities, and an overlying unconformity. Sequence boundaries are recognized by nannofossil biostratigraphic hiatuses, which coincide with hardgrounds, *Glossifungites* ichnofacies, and coarse-grained glauconitic and phosphatic skeletal lags in cores and outcrops. Glauconite-rich beds have regionally extensive log character that overlie angularly truncated section. Facies within sequences can be distinguished as inner ramp (light colored skeletal wackestone, with diverse burrowers and macrofossils), middle ramp (medium gray horizontally burrowed skeletal wackestone), and outer ramp (interbedded dark horizontally burrowed and laminated skeletal wackestone), based on a depositional model of increasing oxygen content in shallower water. Regional cross sections show that the three sequences (AC–I to AC–III) in the Austin Chalk have an extremely asymmetric distribution across the San Marcos Arch. The upper Turonian–lower Coniacian section (AC–I) is very thick west of the San Marcos Arch but is almost completely eroded in the east. The upper Coniacian–Santonian section (AC–II) is very thick east of the San Marcos Arch but is almost completely eroded over the San Marcos arch, and is thin on the west side. The upper Santonian–lower Campanian sequence (AC–III) is more balanced, but similar to the middle sequence. Downdip, the Austin Chalk thins dramatically toward the relict Lower Cretaceous Edwards margin. The Austin Chalk was deposited as a downdip thinning wedge, due to greater carbonate productivity updip and non-deposition or erosion downdip. This interpretation is based on the geometry of the overlying Anacacho Formation, which thickens as the Austin Chalk thins, and internal facies relationships and markers within the Austin Chalk. Petroleum reservoirs in the Austin Chalk occur across a range of inner to outer ramp depositional environments but generally are older on the west side of the San Marcos Arch compared to the east side.

INTRODUCTION

The Austin Chalk has a long history of petroleum production, and it remains the target of active exploration today. Information to describe the Austin Chalk is plentiful, with an outcrop belt that stretches across Texas into Mexico and well logs from tens of thousands of boreholes and numerous cores. An extensive Austin Chalk literature (1950–2022) details the biostratigraphy, lithofacies, and rock properties in outcrop and subsurface. Outcrop studies emphasize lithostratigraphy and biostratigraphy of the chalk, whereas subsurface studies focus on lithofacies, reservoir, and geomechanical properties. However, no regional syntheses on stratigraphy, facies, and depositional environments have been published on this unit yet.

Understanding the stratigraphy of the Austin Chalk is challenging due to the wide thickness variations, from <100–900 ft

Manuscript received June 2, 2023; revised manuscript received August 15, 2023; manuscript accepted August 15, 2023.

GCAGS Journal, v. 12 (2023), p. 45–75.
https://doi.org/10.62371/MBXQ1033

(<30–275 m) along dip and across the San Marcos Arch. Stratigraphic units were first defined in the outcrop (Durham, 1957; Young, 1985), overcoming correlation challenges caused by short, isolated outcrop sections and abundant faults. In the subsurface, petroleum geologists developed an informal nomenclature to describe the stratigraphy (Durham and Hall, 1991; Ewing, 2013; Maranto, 2017), based on log markers that were not readily tied back to outcrop. Subsurface stratigraphic nomenclature differs in the major fields on either side of the San Marcos Arch, due to the difficulty in correlating across the arch as the Austin Chalk thins, and key marker beds pinch out. Unconformities (sequence boundaries) within the Austin Chalk were recognized in outcrop between Austin and San Antonio (Cooper et al., 2020; Durham, 1957; Durham and Hall, 1991; Young, 1985), but they were not recognized in the subsurface (or remained proprietary) until recently (subsurface cross section and maps in Cooper et al. [2020]).

Although the Austin Chalk is dominated by fine-grained carbonate (largely pelagic nannofossils), the lithology, sedimentary structures, and biota vary from updip to downdip and in vertical sequences, indicating a range of depositional environments. Texas was the gateway to the Western Interior Seaway during the Late Cretaceous (Fig. 1), but it differs from the Seaway in having a clearly defined depositional dip direction, enabling lithofacies to be placed in a depositional ramp model.

The Austin Chalk is primarily a lime wackestone with low porosity, with chalky microporosity only occurring in the outcrop and shallow subsurface. As a petroleum reservoir, the Austin Chalk produces from a dual porosity system, with contributions from matrix porosity and natural and induced fractures, in unconventional traps. Studies continue to provide data on how lithofacies, reservoir and geomechanical properties, vertical heterogeneity, and fault networks impact reservoir quality of the Austin Chalk (e.g., Loucks et al., 2020a, 2020b; Zahm, 2020).

This paper describes the regional sequence stratigraphy of the Upper Cretaceous Austin Chalk in South and Central Texas from the outcrop to the downdip limit of well control, based on new nannofossil biostratigraphy, core and outcrop descriptions, wireline log correlations, and literature synthesis. This regional sequence stratigraphic framework ties the stratigraphic nomenclature of the outcrop and the petroleum fields on either side of the San Marcos Arch and places the facies and sequences of the Austin Chalk in context, to better understand the petroleum system and reservoir targets.

GEOLOGICAL SETTING

Sedimentation of the Upper Cretaceous Austin Chalk (Fig. 1) was influenced by the paleobathymetry of the Gulf of Mexico, the Cretaceous Western Interior Seaway, the Llano and Sabine uplifts, and uplifts and basins in Mexico (Blakey, 2013). Sedimentation shifted from Lower Cretaceous shallow water carbonate platforms to Upper Cretaceous pelagic carbonate deposits as sea levels rose (Denne and Breyer, 2016; Ewing, 2016; Goldhammer and Johnson, 2001; Phelps et al., 2014). The shelf edges of the Lower Cretaceous carbonate platforms continued to have topographic expression during Austin Chalk deposition. They form the downdip limit of well control, due to Cenozoic faulting localized downdip from the shelf edges. The Lower Cretaceous platform edges are coincident in Central Texas, but the younger Edwards shelf edge steps back from the Sligo shelf edge in South Texas, forming a submarine shelf or plateau between the shelf margins. Carbonate-rich chalk preferentially accumulated in South and Central Texas, as siliciclastic sediments from the volcanic arc highlands in Mexico were captured in the western foreland basin (Juárez-Arriaga et al., 2019), and siliciclastic sediments from the northeast (Pearson, 2012) were captured in the East Texas Basin. After Austin Chalk deposition, the study area was inundated by Upper Cretaceous siliciclastic sediment from rising uplands in the west (Ewing, 2016).

The Precambrian Llano Uplift is a persistent high that localized continental break-up in the Cambrian, collision in the Pennsylvanian, and break-up in the Triassic (Ewing, 2016). The San Marcos Arch, downdip from Llano Uplift, controlled sediment thicknesses from the Jurassic through the Cenozoic. The original thickness of the Jurassic Louann Salt is reflected by the current distribution of salt diapirs, with only a few in South Texas and none on the San Marcos Arch. The original salt distribution controlled structure and sedimentation through the Cenozoic (Diegel et al., 1995; Fiduk et al., 2009). The San Marcos Arch was not a major uplift in the early Early Cretaceous, based on the relatively straight Sligo shelf edge. It became active before the Edwards Formation was deposited, with southwestward subsidence causing retreat of Edwards shelf edge in South Texas, formation of the Maverick Basin, and differentiation of facies in the basin and on the arch (Phelps, et. al, 2014). Movement of the San Marcos Arch continued to influence sedimentation throughout the Upper Cretaceous (Fig. 2).

Numerous Upper Cretaceous volcanic tuff cones formed in updip areas on either side of the San Marcos Arch (Ewing, 1986, 2004; Thompson, 2019) during Eagle Ford, Austin, and Taylor deposition. Volcanoes in Texas started as phreatic (underwater) tuff cones of alkalic ultramafic composition and grew to be 1 to 2 mi (1.6 to 3.2 km) in diameter and a few hundred feet (60+ m) above the seafloor, becoming subaerial in many cases (Ewing, 1986, 2004). Skeletal packstone and grainstone units that flank many of the volcanoes (Ewing, 1986; Loucks and Reed, 2022; Roy et al., 1981; Thompson, 1986) indicate localized shallower water depths in the Austin Chalk. Other thin volcanic ash beds are interbedded with the Austin Chalk; these are less than an inch to several inches thick (2.5 to 10 cm), regionally correlatable, and contain shards of quartz and plagioclase (Hovorka, 1998) indicating an original rhyolitic or andesitic composition, derived from distant western arc volcanoes (Lee et al., 2018). The regional Austin Chalk isochore map (Fig. 2) shows thinning associated with the San Marcos Arch and Sabine uplift, downdip thinning near the Lower Cretaceous shelf edge in South and East Texas, and a linear thin called the 'Waco Channel' at the eastern edge of the study area. This study address the thickness variations across the San Marcos Arch and downdip toward the Lower Cretaceous shelf edges.

PETROLEUM GEOLOGY

The structural configuration of the Austin Chalk in South and Central Texas is relatively simple (Fig. 3), since the Upper Jurassic Louann Salt is thin to absent over most of the area. Growth faults influenced Austin Chalk deposition at the updip limit of salt, within the peripheral graben system (Atascosa, Karnes, and Milano troughs) and linking en echelon faults (Ewing, 2018). The low amplitude Chittim and Del Rio anticlines formed near the Rio Grande River, at the limit of northeast-directed compressional Laramide tectonics from Mexico during the Eocene (Ewing, 2003). Areas near the Rio Grande and Central Texas Hill Country were uplifted, and Balcones-Luling normal faults formed, during the Oligocene/Miocene (Ewing, 2003; Ewing, 2011, Ewing, 2016).

Petroleum exploration and production in the Austin Chalk moved from updip to downdip over the past 100 yr. The earliest-explored updip trend produced from structural/combination traps around the volcanic tuff cones and the Luling counter-regional faults. Updip reservoirs have up to 20% chalky matrix porosity, low permeability, and high water saturation (Doyle, 1955). At intermediate depths, the Austin Chalk produces from unconventional traps, from Pearsall Field in the west, to Giddings Field in the east. Reservoirs typically have 2–10% porosity and very low permeability (Dawson et al., 1995; Loucks et al., 2020b). Primary

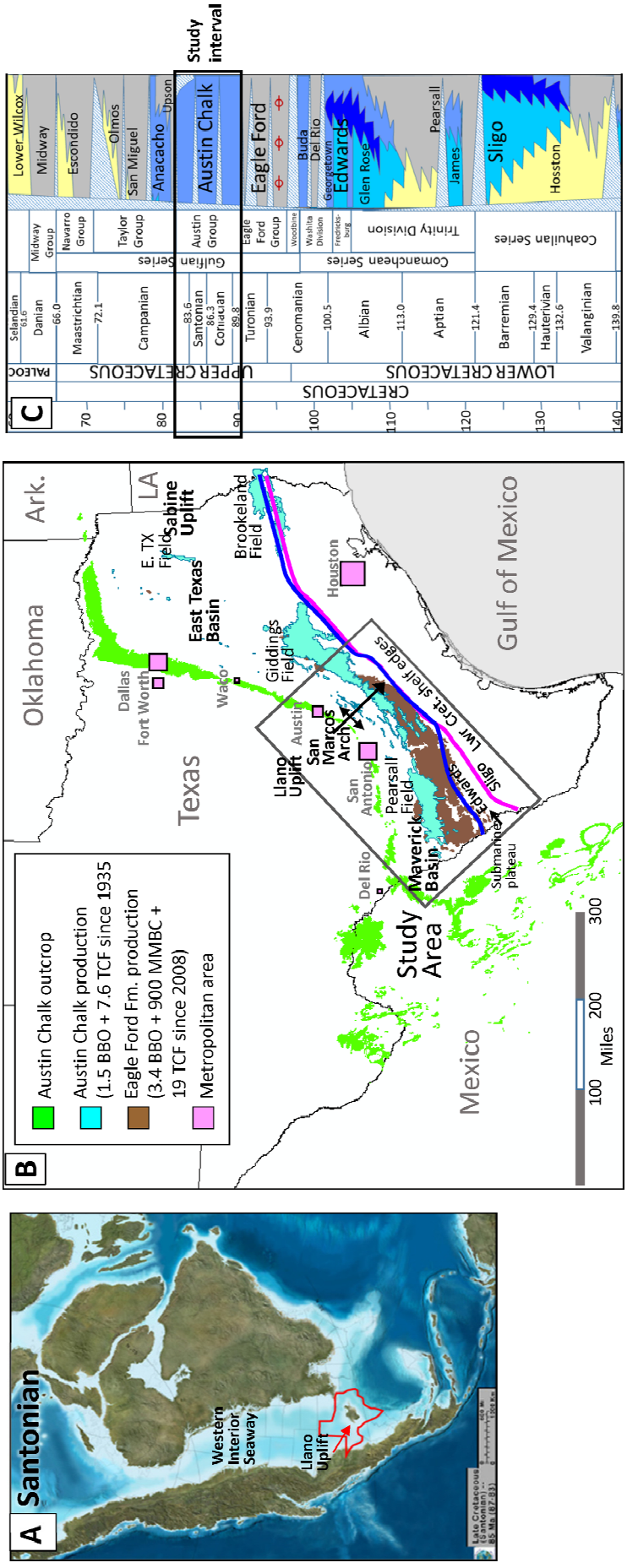

Figure 1. Paleogeographic map, index map, and stratigraphic chart. (A) Santonian paleogeography of North America (reprinted with permission from Blakey [2013]) showing the Western Interior Seaway, the location of Texas, and the Llano Uplift. (B) The index map shows the Austin Chalk outcrops (Texas Water Science Center, 2014; GEOINFOMEX, 2019), the major petroleum fields producing from the Austin Chalk and Eagle Ford Formation (modified after Enverus [2022]) and production data (Enverus, 2022; Texas Railroad Commission, 2022). The black box is the regional study area. Well log data for Austin Chalk is abundant in Texas between the outcrop and Lower Cretaceous shelf edges. No log data is available beyond the shelf edges due to greater depth to the Austin Chalk. C: Stratigraphic chart of the Cretaceous sedimentary section in South Texas (compiled from Ewing [2016], Goldhammer and Johnson [2001], and Phelps et al. [2014]). Dates are from the 2022 International Commission on Stratigraphy (Cohen et al., 2022).

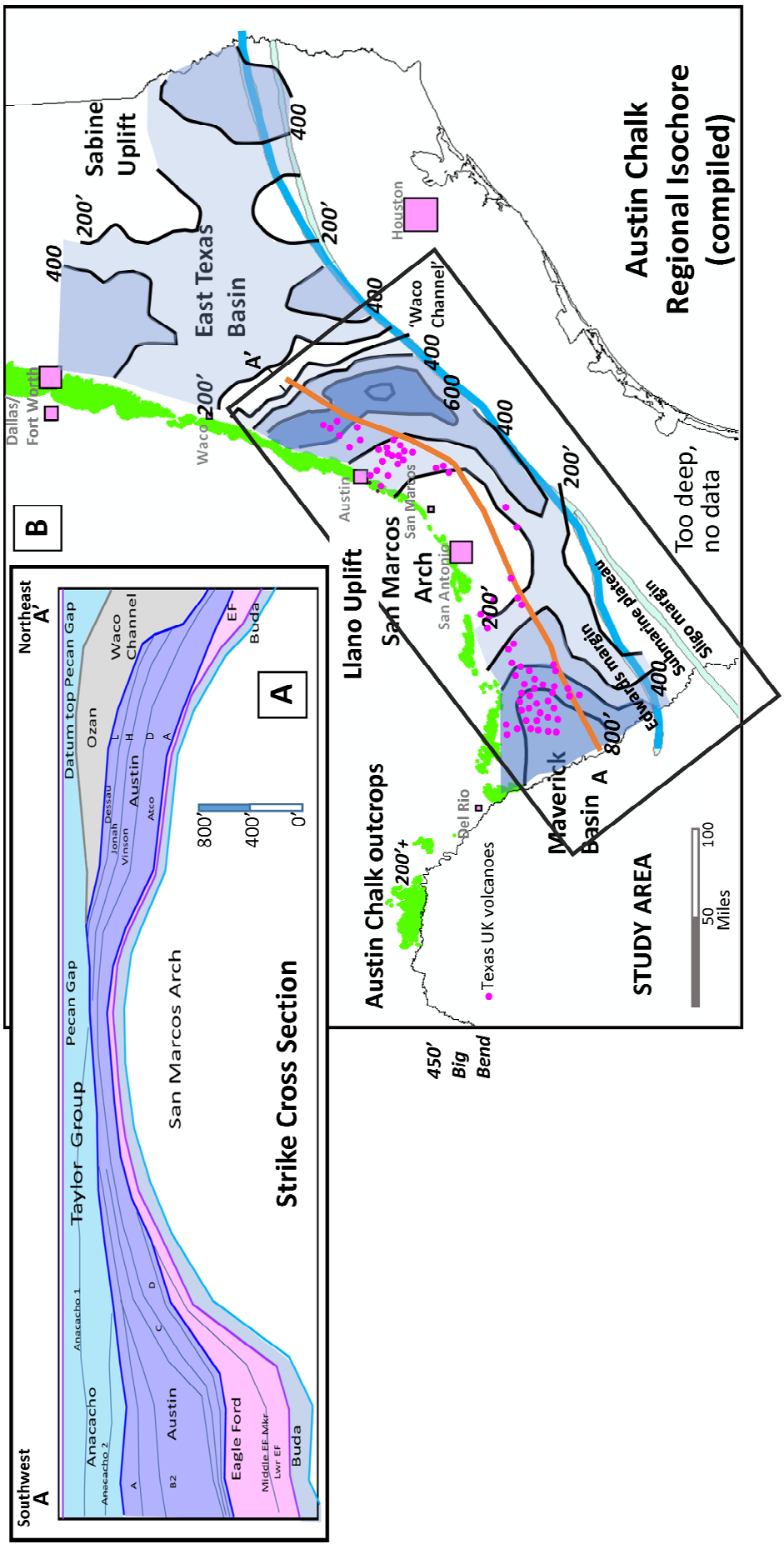

Figure 2. Cross section and regional Austin Chalk isochore. (A) Cross section from South to Central Texas, hung on top of the Anacacho/Pecan Gap formations (modified after Ewing [2016]). (B) Regional Austin Chalk isochore map (compiled from Cooper et al. [2020], Ewing [2013], Holifield [1982], Koger [1981], and Short [2018]). Magenta circles are Upper Cretaceous volcanoes (from Ewing et al. [1990]).

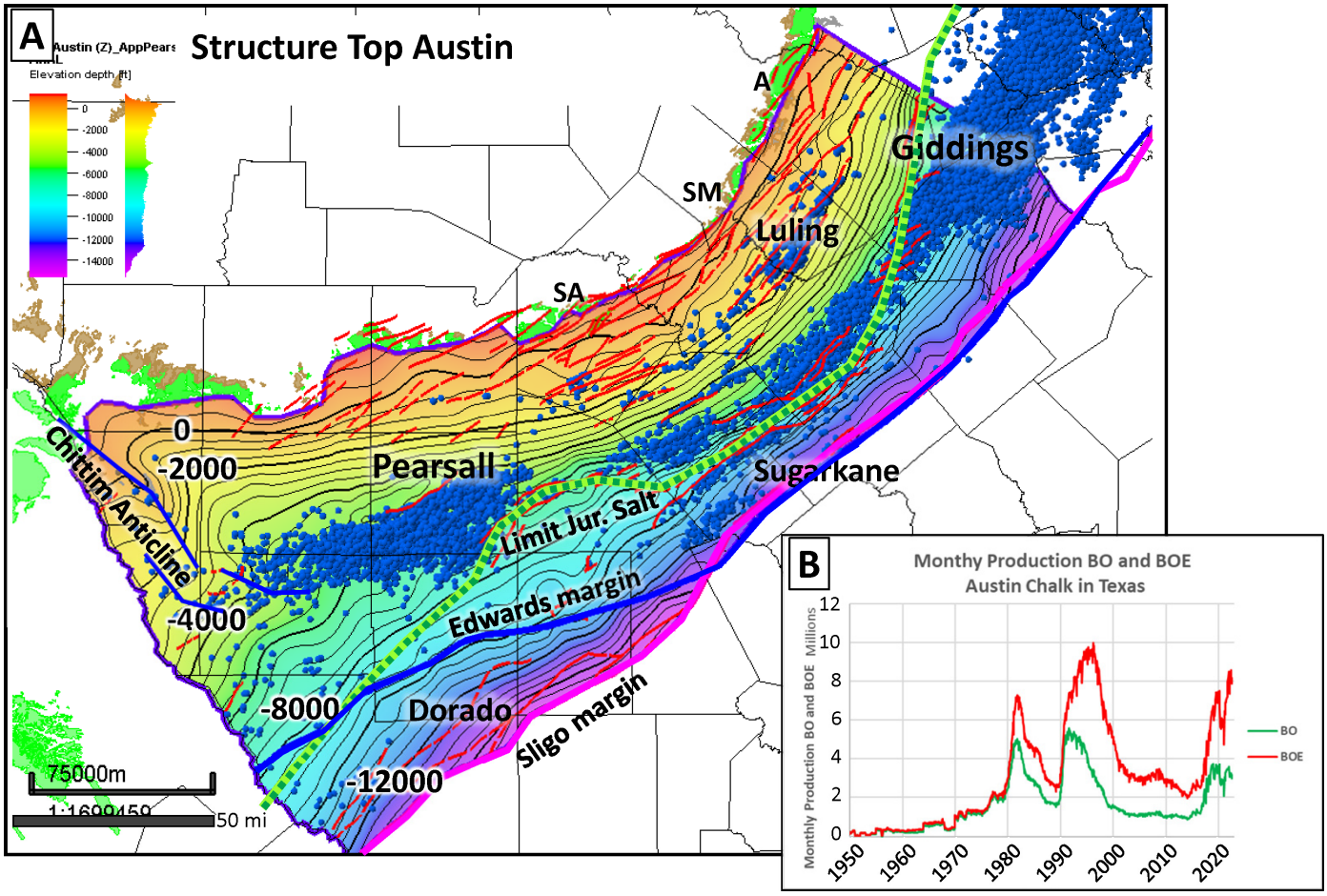

Figure 3. Top Austin structure map and production history. (A) The Austin Chalk structure map shows a very broad San Marcos Arch and uplift near the Rio Grande River. Lines show Jurassic salt limit and Lower Cretaceous shelf edges. Productive Austin Chalk wells (data from Enverus [2022]) are overlain on the Austin Chalk structure map. The Austin Chalk produces from updip structural-stratigraphic traps, and unconventional traps enhanced by a nose at Pearsall Field, and faulted homoclinal dip at Giddings Field. (B) History of Austin Chalk production in Texas (data from Enverus [2022]) shows three main times of increased production in Austin Chalk. Gas has become an increasingly important objective through time, as seen from larger production of barrels of oil equivalent (BOE) relative to barrels of oil (BO).

reservoir facies are clean carbonate with few interbedded marl beds, prone to fracturing. The middle and upper portion of the Austin Chalk is the most productive reservoir in Pearsall Field (Ewing, 2013), and the lower portion of the Austin Chalk is the most productive reservoir in Giddings Field (Holifield, 1982; Maranto, 2017). Vertical wells from the early 1980s targeted fractured areas enhanced by broad arching over Pearsall Field or small normal faults in Giddings Field. Horizontal wells drilled after the late 1980s targeted more fracture-prone reservoir intervals to intersect and link multiple fracture sets.

Recent Austin Chalk development is downdip, in relatively thick Austin Chalk on either side of the Edwards shelf margin, above Eagle Ford productive wells (Enverus, 2022). Landing zones for horizontal wells tend to be in the middle portion of the Austin Chalk in South Texas and in the lower portion in Central Texas. Despite relatively low matrix porosity and few natural fractures, reservoirs can be very productive with modern hydraulic fracturing techniques in the light oil, wet gas, and dry gas trends (Darbonne, 2020; Maranto, 2017; Pickett, 2018). Production may be enhanced near faults, either due to improved matrix porosity caused by diagenesis (Dravis, 2018) or enhanced fracturing (Male and Zahm, 2021).

PREVIOUS WORK

Stratigraphy

Early studies (Stephenson, 1937; Taff, 1892) recognized multiple lithostratigraphic units (Fig. 4) in the Austin Chalk outcrop belt based on lithologic and faunal variations. Detailed outcrop study (Durham, 1957) distinguished six lithostratigraphic units: the Atco, Vinson, Jonah, Dessau, Burditt, Big House (now called Pflugerville) units, from the bottom up. The Austin Chalk is now considered a group in the type area, with six formations, having the type sections near Austin (Young, 1985), where the total Austin Chalk thickness is ~400 ft (~122 m) (Lundquist, 2015a).

A major unconformity (Fig. 4) was recognized within the Austin Chalk (Durham, 1957) between Austin and San Antonio. The unconformity occurs below the Dessau Formation, with angular truncation cutting the Jonah Formation and most of the Vinson Formation toward San Antonio. Correlations in outcrop are based on hard grounds and firm grounds at the unconformity surface, glauconitic packstone above the unconformity and persistent fossiliferous beds in overlying and underlying formations. Smaller disconformities, with similar characteristics, occur with-

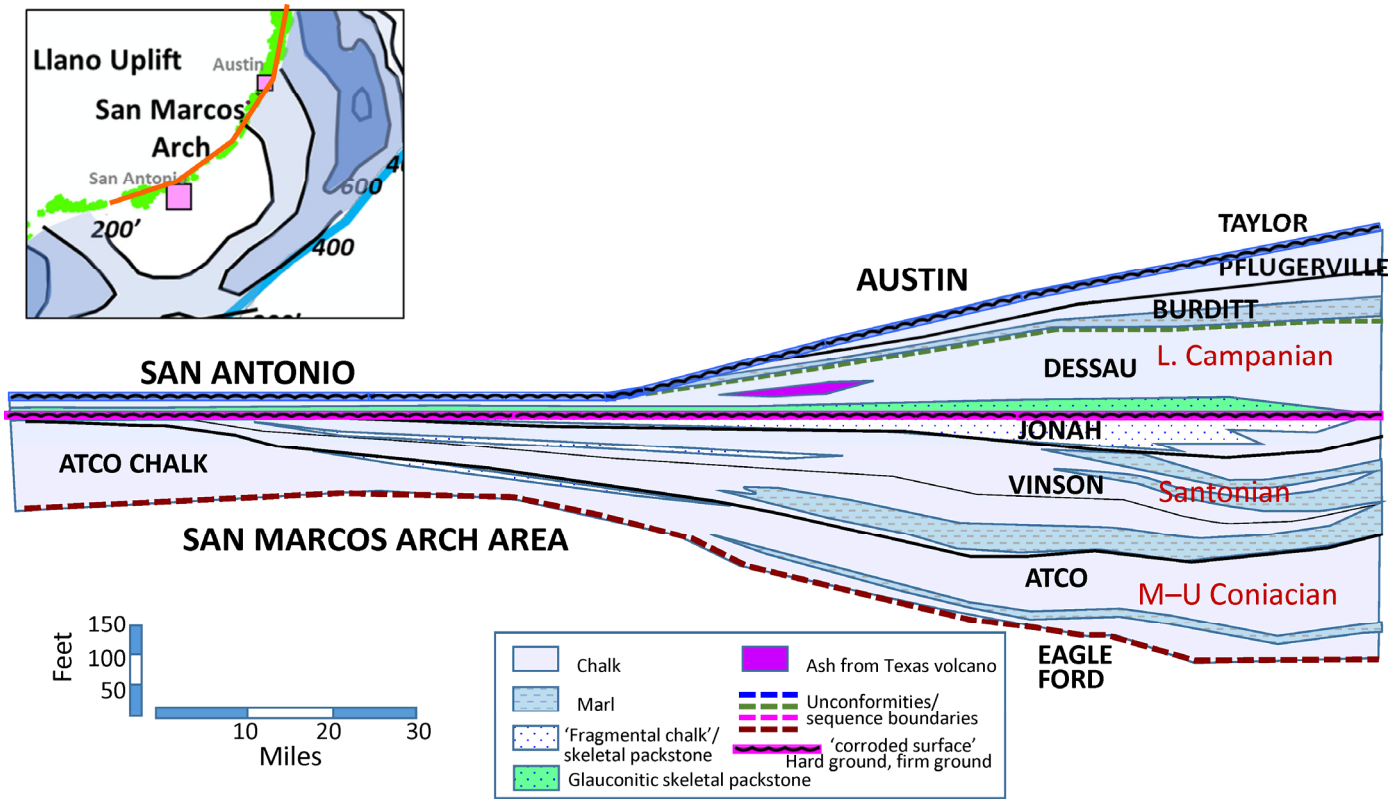

Figure 4. Lithostratigraphic cross section of the Austin Chalk in outcrop from San Antonio to north of Austin (adapted from Durham [1957]). Six formations are recognized in the Austin Chalk in outcrop near Austin. Major unconformities occur at the base, middle and top of the Austin Chalk. The Austin Chalk formations thin and are truncated from northeast to southwest, toward San Antonio. Ties to Cretaceous stage names are from ammonites (Young, 1985) and nannofossils (Jiang, 1989).

in or between other formations. An unconformity at the top of the Austin Chalk cuts the Pflugerville, Burditt, and most of the Dessau formations toward San Antonio and is recognized by a bored hardground overlain by phosphatic nodules. The section is less than 170 ft (50 m) thick in San Antonio (Cooper et al., 2020). The Atco Formation makes up most of the Austin Chalk section in San Antonio. The thin Vinson and Jonah formations are overlain unconformably by a 5 ft (1.5 m) thick Dessau Formation, which is overlain unconformably by Taylor Group marl. The San Antonio outcrop was tied to the subsurface (Cooper et al., 2020), using outcrop gamma ray (GR) measurements tied to GR logs in shallow wells. A cross section between San Antonio and Austin shows the major unconformities in the middle and at the top of the Austin Chalk,

Subsurface stratigraphy is based on wireline log markers from GR, spontaneous potential (SP), and resistivity logs. Austin Chalk nomenclature differs across the San Marcos Arch as log markers pinch out over the arch and have different characteristics on either side (Fig. 2A). The stratigraphic nomenclature in Pearsall Field west of the arch goes from A to E, with A at the top (Ewing, 2013). The stratigraphic nomenclature in Giddings Field east of the San Marcos Arch goes from A–M, with A at the base (Maranto, 2017).

Biostratigraphy

The Austin Chalk is correlated into the international time scale through multiple fossil groups (Fig. 5), although this tie has evolved through the years, as the understanding of species and the definition of stages and dates have changed. Most of the biostratigraphic data for the Austin Chalk is from outcrop studies near Austin. The six formations in the chalk can be distinguished and tied to the international scale based on ammonites, inoceramids, and other molluscs (Cobban et al., 2008; Young, 1985), crinoids (Gale et al., 1995), foraminifera (Alshuaibi, 2006; Corbett et al., 2014; Lowery, 2013; Lundquist, 2015a; Pessagno, 1969), and nannofossils (Corbett et al., 2014; Jiang, 1989). Several integrated biostratigraphic studies on the Austin Chalk outcrops near Dallas support proposed global boundary stratotype sections and points (GSSP) (Gale et al., 2008; Gale et al., 2007) or tie into regional biostratigraphy (Hancock and Walaszczyk, 2004). Published Austin Chalk biostratigraphy in the subsurface is limited to the short sections just above Eagle Ford analyses (i.e., Corbett et al., 2014; Denne et al., 2016).

Nannofossils have relatively good stratigraphic resolution in the Austin Chalk. Jiang (1989) distinguished six nannofossil assemblages, which roughly correspond to the six formations in the Austin Chalk outcrop. He applied the cosmopolitan biostratigraphic zonation of Sissingh (1977) with some minor modifications. The scheme uses numbered CC (Cretaceous coccolith) zonations, which are commonly are employed in Eagle Ford Group and Austin Chalk biostratigraphy (e.g., Corbett et al., 2014; Denne et al., 2016; Gale et al., 2008; Gale et al., 2007; Jiang, 1989). A number of nannofossil biostratigraphers have documented problems with the CC zones due to variable fossil distribution, preservational factors, and changing species concepts (i.e., Bralower and Bergen, 1998; Bergen and Sikora, 1999; Corbett et al., 2014). The Austin Chalk studied here includes zones CC13–CC18a, but the delineation of zones CC15 and CC16 are particularly problematic. The event used to define the Zone CC15/CC16 boundary in the Santonian is the lowest occurrence (LO) *Lucianorhabdus cayeuxii* (Sissingh, 1977). Because

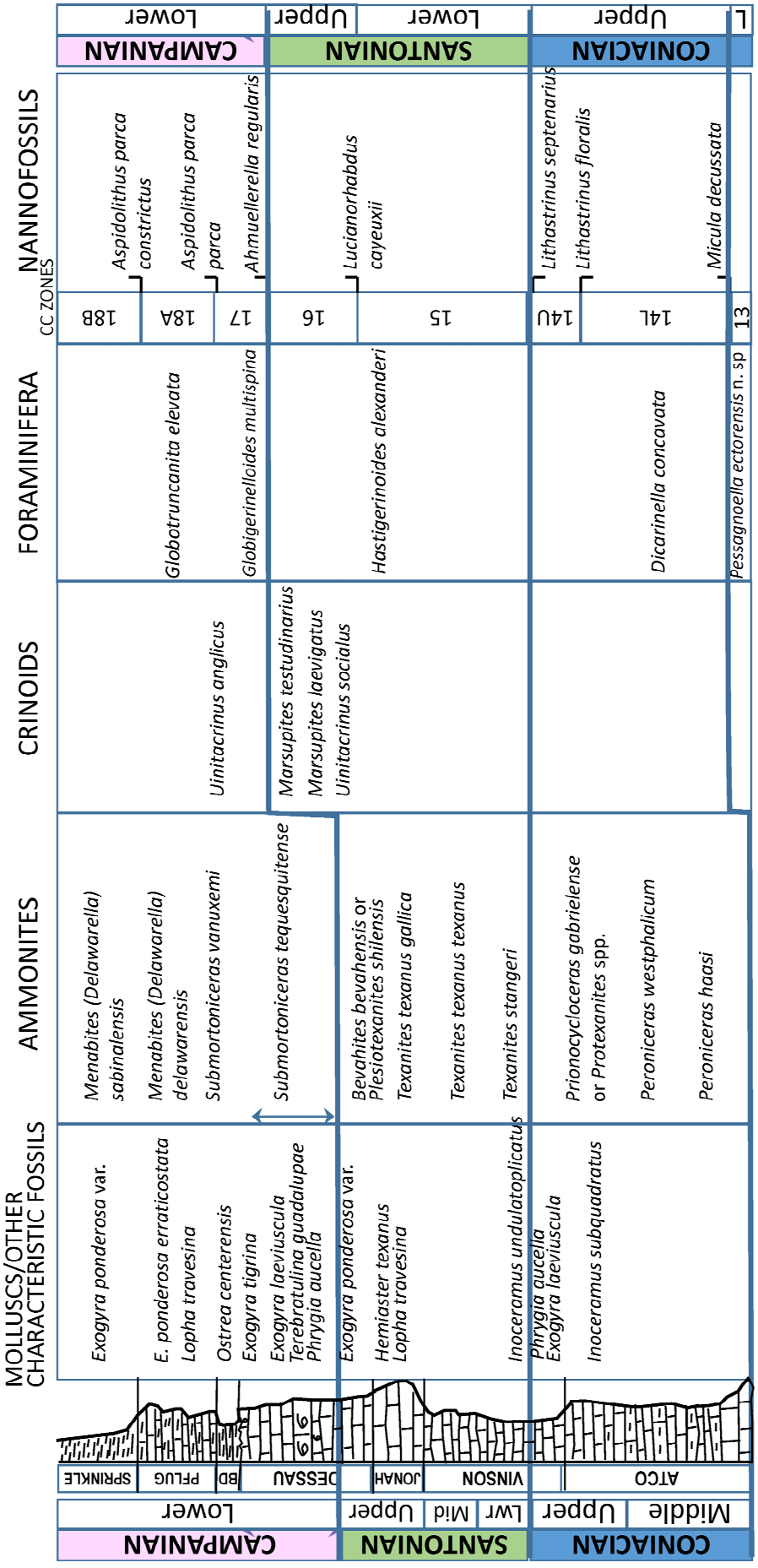

Figure 5. Biostratigraphic index fossils in the Austin Chalk. Composite stratigraphic section of the Austin Chalk from near the city of Austin (adapted from Young [1985]), with the index fossils for each lithostratigraphic unit. Authors are listed at the base of each column. The boundary between the Coniacian and Santonian, within the lower Vinson Formation, is consistently picked on multiple index fossils. The boundary between the Santonian and Campanian changed from the lower Dessau to the upper Dessau in recent years, as new criteria emphasized crinoids and nannofossils over ammonites. The nannofossil chart from Jiang (1989) is slightly different than the one used in this study (see Figure 10).

of inconsistencies with the lower range of this taxon and difficulties distinguishing it from *L. maleformis* in poorly preserved specimens (e.g., see Bralower and Bergen [1998]), it was not used to subdivide these zones in this study.

The International Commission on Stratigraphy (ICS) has produced multiple versions of the international time scale in recent years (Gale et al., 2020; Ogg and Hinnov, 2012; Ogg et al., 2016). Ammonite, inoceramid, and foraminiferal biostratigraphy are relatively consistent from the Turonian through the Campanian in sequential versions of the stratigraphic chart. Nannofossil zones, however, differ considerably from one version to another, having different durations and moving across stage boundaries, making it challenging to communicate and to use previous schemes. The absolute ages of Late Cretaceous boundaries also vary, based on latest research on dates and evolving concepts in stratigraphy (Gale et al., 2020; Ogg and Hinnov, 2012; Ogg et al., 2016). This study uses the absolute dates from the 2012 time scale (Ogg and Hinnov, 2012), since nannofossil zonations are similar to the Austin Chalk outcrop biostratigraphy from Jiang (1989) and the ICS (2022) web version of International Chronostratigraphic chart (Cohen et al., 2022), and because the documentation is not clear about why dates for the base and top Santonian were shifted in the 2016 and 2020 time scales.

Facies, Depositional Models, and Sequence Stratigraphy

The Austin Chalk is a pelagic deposit containing nanno-size coccoliths, silt-size pelagic foraminifera and calcispheres, and larger macrofossils (Dravis, 1980, 1991; Loucks et al., 2020b, 2021a, 2021b). Facies are generally skeletal wackestone, but vary from highly burrowed to laminated, from clean to argillaceous or organic-rich carbonate, and have variable quantities and types of macrofossils. Units often are cyclic, alternating between chalk and marl. Sedimentary structures range from complete burrow homogenization (massive bedding) to complex burrow tiering to sparsely bioturbated to finely laminated (Zheng et al., 2021, in press), depending on benthic oxygen conditions. The Austin Chalk in the subsurface is interpreted as deposited in a shelf setting below wave base (Loucks et al., 2020b), having less oxygen and more organic and siliciclastic content downdip (Dravis, 1980; Grabowski, 1995). Further updip, the outcrop is interpreted to be nearer fair water wave base (Cooper et al., 2020; Dravis, 1980; Loucks et al., 2020b).

Unconformities were recognized in outcrop studies (Cooper et al., 2020; Durham, 1957; Stephenson, 1937; Young, 1985), based on hardgrounds and firmgrounds, underlain by angularly truncated beds and overlain by glauconitic or phosphatic packstone. Nannofossil biostratigraphy along outcrop belt (Jiang, 1989) showed angular truncation at the base, middle and top of the Austin Chalk, with longer hiatuses toward San Antonio. The first sequence stratigraphic interpretation of the Eagle Ford and Austin Chalk (Jiang, 1989) was based on lithostratigraphic and nannofossil biostratigraphic tied to global sea level curves (Haq et al., 1987).

A recent detailed surface-to-subsurface sequence stratigraphic framework was created for the Austin Chalk in the greater San Antonio area (Cooper et al., 2020). Water depths were interpreted from sedimentary textures and skeletal abundance, with more abundant and diverse macrofossils and burrowers in shallower water facies. Sequence boundaries were based on glauconitic or phosphatic lags overlying hardgrounds, firmgrounds, and skeletal packstone beds. Maximum flooding surfaces were recognized as foraminiferal wackestone or marl beds between coarser-grained or more heavily burrowed chalk units. Outcrop GR measurements, tied to shallow well logs, identified sequences and system tracts in the subsurface between San Antonio and Austin. Highstand tracts are characterized by low GR and negative SP values (clean chalk). Transgressive units and maximum flooding surfaces have higher GR and no SP development, due to increased clay content. The lithostratigraphic formations of the Austin Chalk outcrop generally are clean carbonates, recognized by low GR or negative SP in subsurface logs, and are separated from one another by higher GR intervals. A subsurface cross section paralleling the outcrop belt (Cooper et al., 2020) showed major unconformities in the middle and at the top of the Austin Chalk.

Other large-scale depositional architecture occurs in the Austin Chalk (Fig. 2). Downdip thinning and low angle carbonate clinoforms were described in South Texas in the Pearsall Field area (Ewing, 2013). A linear thin, called the Waco Channel (Fig. 2) occurs at the eastern edge of the study area. It extends from the outcrop near Waco to the Edwards shelf edge. The upper and middle Austin Chalk is missing within the channel, due to submarine erosion (or non-deposition). The channel is filled by lower Campanian Ozan Formation shale (e.g. Holifield, 1982; Durham and Hall, 1991; Hayes, 2021).

DATA AND METHODS

This regional study covers an area of 250 miles by 75 miles (400 x 120 km), across 27 counties, from the Rio Grande to Austin, and from the outcrop belt to the limit of well data at the Lower Cretaceous shelf margins (Fig. 6). Over 600 well logs from S&P Global (formerly IHS Markit), Enverus DrillingInfo, MJ Logs, Texas Bureau of Economic Geology (BEG), Texas Water Development Board, U.S. Geological Survey, and from energy companies were used in this study. The main wireline logs used for correlation were GR, SP, and resistivity. Schlumberger's Petrel® software was used to correlate well logs and make cross sections and maps.

Cores were chosen for completeness and distribution across the study area. Cores included several proprietary cores from energy companies, and publicly available core from the BEG and U.S. Geological Survey (Table 1). Bed-by-bed descriptions include texture, fabric, mineralogy, color, bed boundaries, sedimentary structures, bioturbation, and fauna. Thin sections were made from some cores; the BEG made thin section photos available from other cores. Descriptions were collaborated with x–ray fluorescence (XRF) measurements. Core descriptions from theses and publications (Dravis, 1980; Grabowski, 1981; Hayes, 2021; Hendrix, 2016; Loucks et al., 2020a, 2020b; Loucks and Reed, 2022) were incorporated in the study (Appendix A in Griffith [2023]). Multiple Austin Chalk outcrops were visited between Terrell and McLennan counties. Several outcrops in South Texas, including Lozier Canyon and Langtry, were measured, and spectral GR values were acquired (Griffith et al., 2019). Measured sections from theses and publications (Cooper et al., 2020; Corbett et al., 2014; Durham, 1957; Jiang, 1989; Lundquist, 2001, 2015a, 2015b; Young, 1985; Young et al., 1977) also were incorporated in the study. EasyCore® was used to integrate core and outcrop photos and descriptions with biostratigraphy, XRF measurements, and wireline logs.

Nannofossil samples from two cores having complete penetration of the Austin Chalk interval were collected from either side of the San Marcos Arch. The Getty Lloyd Hurt #1 (4228330305, total depth [TD] 7239 ft [2206 m], La Salle County) is west of the arch and has 482 ft (147 m) of Austin Chalk. The Shefts Sallie Clark #1 (4205501852, TD 2221 ft [677 m], Caldwell County) is east of the arch and has 280 ft (85 m) of Austin Chalk. James Pospichal analyzed nannofossils in these two wells (Appendix B in Griffith [2023]). He also analyzed samples from several other cores covering the Eagle Ford / Lower Austin Chalk contact, including a 'well Y' in Karnes County and three wells in Webb County (Corbett et al., 2014). Eric de Kaenel analyzed nannofossil samples from the Tesoro Valcher #1 (4249330230, TD 7008 ft [2136 m], Wilson County) with 145 ft (44 m) of Austin Chalk (Appendix B in Griffith

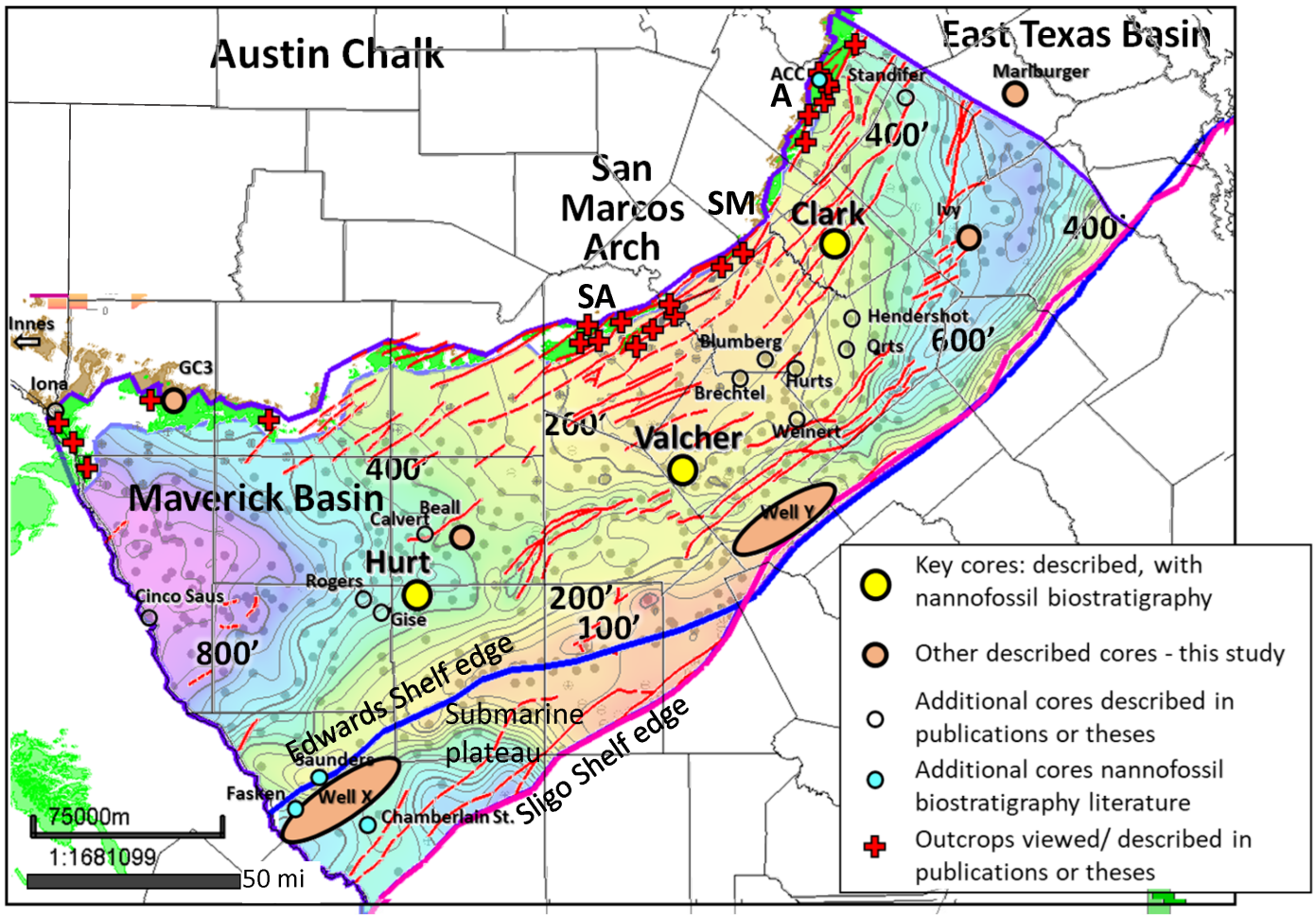

Figure 6. Austin Chalk isochore map with correlated well logs used in the study. Faults (red lines) are from Ewing et al. (1990). SA, SM, A are the locations of San Antonio, San Marcos, and Austin, respectively. Major thinning occurs over the San Marcos Arch between San Antonio and San Marcos. Overlay shows Austin Chalk cores and outcrops in study area. Yellow and brown circles and ovals are cores described as part of this study (and by Conte [2020], Hayes [2021], and McCreary [2022]). The three large yellow circles have new nannofossil biostratigraphic data from James Pospichal and Eric de Kaenel. Small aqua circles have published nannofossil biostratigraphy (Corbett et al., 2014). Small white circles are from cores described in the literature (Dravis, 1980; Grabowski, 1981; Hayes, 2021; Hendrix, 2016; Loucks et al., 2020a, 2020b, 2021a; Loucks and Reed, 2022; Minisini et al., 2018; Phelps et al., 2014; Zheng et al., 2021). Red crosses show visited outcrops and measured sections from literature (Cooper et al., 2020; Dravis, 1980; Durham, 1957; Durham and Hall, 1991; Ferrill et al., 2020; Jiang, 1989; Minisini et al., 2018; Young, 1985, 1986; Young et al., 1977). The Shell Innes core, near the US90 Langtry outcrop, is just beyond the western edge of study area (Corbett et al., 2014; Griffith et al., 2019; Minisini et al., 2018).

[2023]). This core on the San Marcos Arch is a nearly complete Austin Chalk penetration. John Cooper collected samples from this core, and Alexis Godet from the University of Texas at San Antonio shared the analysis. James Pospichal integrated the results from these wells with the outcrop biostratigraphy (Jiang, 1989) and with the global time scale.

RESULTS

Log correlations were the starting point for this study. Correlations are readily made in South and Central Texas where the Austin Chalk is thick, but the correlations become difficult where the chalk thins over the San Marcos Arch. Biostratigraphy, integrated with core and outcrop descriptions, was essential to correlate across the San Marcos Arch and onto the submarine plateau. This paper discusses how facies and correlations fit into the sequence stratigraphic interpretation. A follow-up paper in preparation will show more detailed cross sections and maps.

Core availability limits full understanding of facies variability in the Austin Chalk. Most of the available cores are from the historically most productive portions of the Austin Chalk: the middle and upper portion in Pearsall Field and the lower portion in Giddings Field. Cores from the Eagle Ford Group trend only include the lowermost Austin Chalk. Cores were not available to describe the middle and upper portions of the Austin Chalk downdip and toward the east.

Lithofacies

Description

The Austin Chalk is interpreted to be like other formations in the Gulf Coast, deposited on a gentle slope that dips toward the Gulf of Mexico. Updip and downdip facies differ because they occupy different places on the depositional profile. Vertical trends also provide information about lateral facies changes.

The facies in the Austin Chalk are placed in a sequence stratigraphic framework, based on recognition of updip and downdip facies, sequence boundaries, and flooding surfaces. Two types of facies are distinguished: facies that represent normal

Table 1. Austin Chalk cores described as part of this study.

Well Name	API	County	TD	Core Depths	Ages Penetrated	Data	References
Getty Hurt #1	42283303050000	LaSalle	7239 ft	6735–7304 ft	Lwr Anacacho; Full Austin (482 ft); Upr EF (87 ft)	Description, XRF, TOC, mineralogy, nannofossil biostrat	Loucks et al. (2020a); Loucks et al. (2020b); Grabowski (1981); McCreary (2022)
Getty Beall #1	42163302920000	Frio	6217 ft	5610–5773 ft; 5920–5980 ft	B–Pflug–Upr Atco (163 ft); Lwr Atco (60 ft)	Description	Dravis (1980); Grabowski (1981)
Tesoro Valcher #1	42493302300000	Wilson	7008 ft	6660–6805 ft; 6875–6960 ft	Dessau, Upr–Lwr Atco (145 ft); EF gap in core; Buda (85 ft)	Description, nannofossil biostrat	Hendrix (2016), XRF; Loucks and Reed (2022)
Shefts Sallie Clark #1	42055018520000	Caldwell	2221 ft	1876–2210 ft	Lwr Aacacho (16 ft); Full Austin (280 ft); EF (17 ft); Buda (21 ft)	Description, XRF, nannofossil biostrat	Loucks and Reed (2022); McCreary (2022)
Well X	proprietary	Webb			Lower Austin (130 ft); Full EF and Buda	Description, XRF, limited nanno biostrat	
Well Y	proprietary	Karnes			Lower Austin (62 ft); Full EF	Description, XRF, limited nanno biostrat	Conte (2020)
USGS GC-3	Shallow corehole	Kinney	500 ft	19–63 ft Austin; 63–500 ft	Lower Austin (44 ft); Full EF and Buda, and Del Rio; top Georgetown	Description, XRF, limited nanno biostrat	
Shell Innes	Shallow corehole	Val Verde	377 ft	9–84 ft Austin; 84–377 ft EF	(Lwr Austin) Lwr Atco (75 ft); Full EF; most of Buda	Description, XRF, TOC, Min, biostrat, dated ashes	Minisini et al. (2018)
Shell Iona	Shallow corehole	Kinney	584 ft	10–130 ft Austin;130–584 ft EF	(Lwr Austin) Lwr Atco' base Upr Atco (120 ft); Full EF; top Buda	Description, XRF, TOC, Min, biostrat, dated ashes	Minisini et al. (2018)
Cities Service Ivy #1B	42149305680000	Fayette	8520 ft	8304–8505 ft	201 ft Lower Austin Atco/ Vinson	Description	Hays (2021)
Prairie Marburger #1	42287300460000	Lee	7245 ft	6867–6987 ft	120 ft Lower Austin Atco/ Vinson	Description, XRF	Hendrix (2016); Hays (2021)

sedimentation within a sequence, and facies that have sequence stratigraphic significance (thin regionally extensive beds).

Most of the facies from within sequences (Fig. 7) are very extensive, but some only occur in particular settings. The updip depositional settings of the Austin Chalk include the outcrop belt, the shallow San Marcos Arch, and areas around the Texas volcanic tuff cones. Updip facies (facies A–D) have macrofossils like oysters and echinoids and are well bioturbated, to the point of being nearly massive. These facies are porous, with preserved chalky microporosity (Dravis, 1980), due to limited burial. They have light colors, from white to light gray to buff. XRF data (McCreary, 2022) indicates chalk beds are characterized by a high proportion of Ca, with the interbedded marl beds having more Si, Al, and K. Carbonate-rich chalk intervals typically have a negative SP and low GR log character. Resistivity values are low in updip areas, indicating a porous and wet reservoir.

Facies A: Coarse-grained skeletal packstone/grainstone (Fig. 7A), containing fragmented red algae, inoceramids, oysters, and echinoids in a massive fine-grained matrix. This facies was only observed in the Tesoro Valcher well, which is located 2.5 mi (4 km) southwest of the several hundred foot (<100 m) high Sutil tuff cone (Ewing, 1986). This coarse-grained facies is described around other Texas volcanic tuff cones (Loucks and Reed, 2022; Roy et al., 1981; Thompson, 1986; Young, 1985). It is recognized in logs by a well-developed negative SP, low GR, and moderate resistivity values. The underlying tuff cones have positive SP, low-medium GR, and low resistivity values, and are recognized by their anomalous geometry interrupting the normal stratigraphy.

Facies B: Medium grained skeletal packstone (Fig. 7B). This facies consists of closely packed fragments of inoceramids, oysters, echinoids, gastropods, and foraminifera in a fine-grained matrix. This facies is characteristic of the Jonah Formation in outcrop (Durham, 1957; Young, 1985) and intervals in the Upper Atco in San Antonio (Cooper et al., 2020).

Facies C: Oyster packstone (Fig. 7C). Closely packed whole or fragmented oysters in a fine-grained matrix, in 1–5 ft (0.3–1.5 m) thick beds. This facies is regionally extensive as biostromes and enables correlation of outcrop sections from the Upper Atco through Pflugerville Formation (Cooper et al., 2020; Durham,

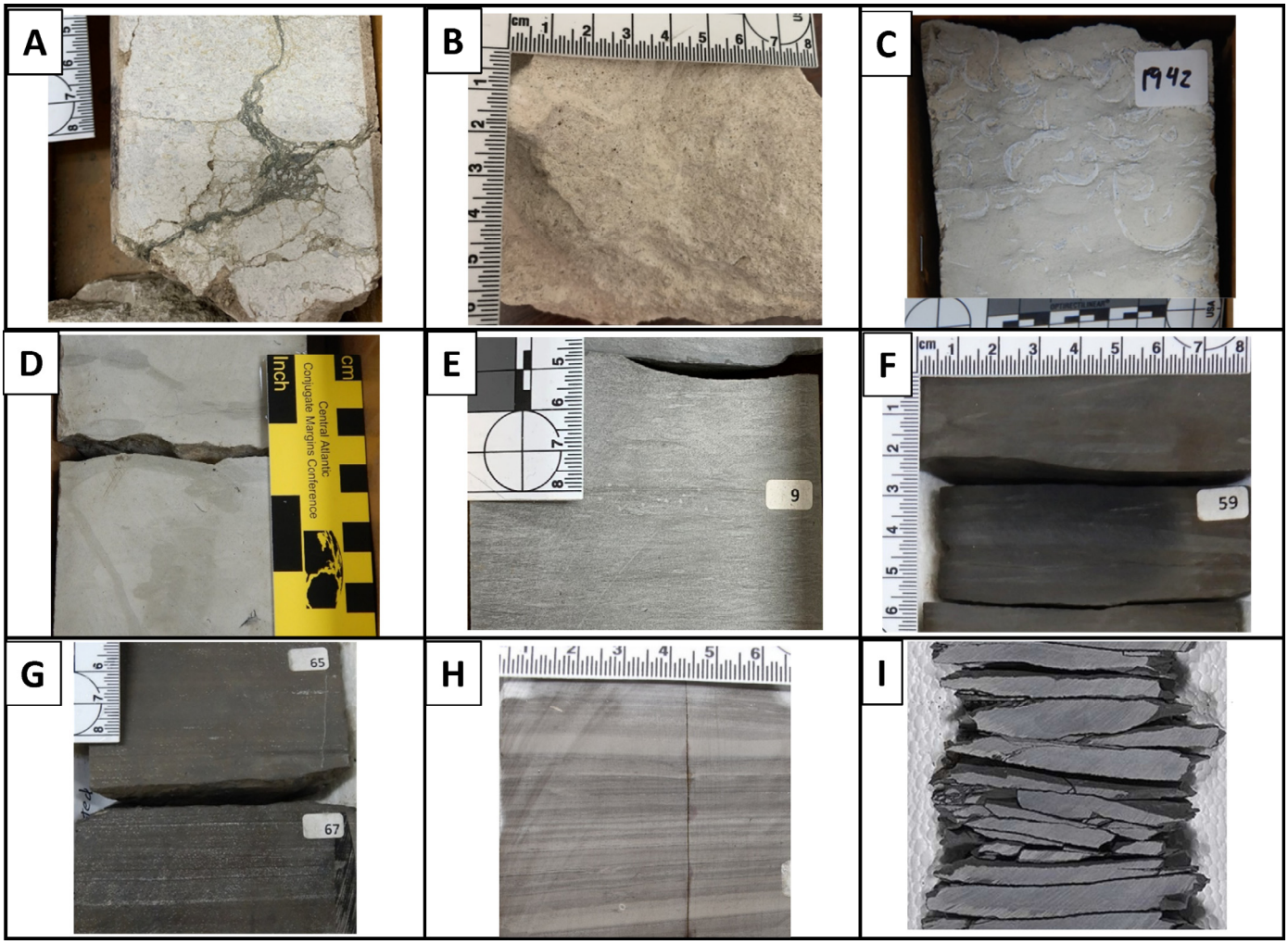

Figure 7. Austin Chalk facies, from inner to outer ramp. (A) Coarse-grained red algal packstone above local Texas volcanic tuff, possible karst exposure, Tesoro Valcher, 6682 ft (2037 m), Lower Atco Fm., lower 'B–2' interval, AC–I. (B) Medium-grained inoceramid and oyster fragmental packstone, outcrop sample, Cathedral Rock Park, San Antonio, Upper Atco Fm., AC–II. (C) Oyster packstone, Shefts Clark, 1942 ft (592 m), Dessau Fm., AC–III. (D) Light colored variably burrowed skeletal wackestone, Shefts Clark, 2127 ft (648 m), Upper Atco Fm., AC–II. (E) Medium gray horizontally burrowed wackestone, Tesoro Valcher, 6734 ft (2053 m), Lower Atco Fm., AC–I. (F) Dark gray-brown horizontally burrowed wackestone, ~2% TOC, Getty Lloyd Hurt, 6987 ft (2130 m) Lower Atco Fm., lower 'B–2' interval, AC–I. (G) Dark gray-brown laminated foraminiferal wackestone, ~2% TOC, Getty Lloyd Hurt, 7096 ft (2163 m), Lower Atco Fm., upper 'D' interval, AC–I. (H) Medium gray laminated and layered skeletal wackestones, City Service Ivy, 8385 ft (2556 m), Upper Atco Fm., AC–II. (I) Splintered medium gray skeletal wackestone, horizontal fabric, no sedimentary structures, well X, Webb County, Atco Fm., AC–II.

1957; Young, 1985). Subsurface examples occur in the Shefts Sallie Clark #1, on the east flank of the San Marcos Arch.

Facies D: Skeletal wackestone, light-colored, with diverse or large burrows or homogenized sediment (Fig. 7D). Sparse inoceramid fragments and oysters occur together with pelagic foraminifera and calcispheres in a fine-grained matrix. This is the most common facies in updip settings. Thin interbedded marl (argillaceous skeletal wackestone) beds become more frequent downdip from the San Antonio outcrop.

Downdip facies (facies E–I) are dominated by horizontal burrowers or are laminated. They have darker colors than updip facies, due to more admixed argillaceous material, disseminated pyrite, or organic matter. Carbonate-rich chalk intervals have a negative SP and low GR log character, with relatively higher resistivity values, due to organic matter, oil saturation, or tight reservoir.

Facies E: Skeletal wackestone, medium-dark grey, with pervasive horizontal burrows or homogenized sediment (Fig. 7E). This is a common background facies for much of Austin Chalk deposition and often is interbedded with thin marl beds.

Facies F: Skeletal wackestone facies, brownish gray, with sparse horizontal burrows (Fig. 7F), with ~2% organic matter (Loucks et. al, 2020b). This is a characteristic facies in the Lower Austin 'C' and 'D' marker beds and is interbedded with other facies in the 'D' interval in the Getty Lloyd Hurt well in Pearsall Field. This facies has high GR (high U on spectral GR) and medium to high resistivity values.

Facies G: Skeletal wackestone, dark grey to brownish gray, laminated (Fig. 7G), with ~2% organic matter (Loucks et. al, 2020b). Laminations consist of millimeter-scale foraminifera or concentrations of organic matter. This facies is characteristic of the Lower Austin 'C' and 'D' intervals in the Getty Lloyd Hurt well and is thinly interbedded with horizontally burrowed facies.

Facies H: Medium gray skeletal wackestone facies that is layered on a centimeter-scale rather than laminated on a millimeter-scale (Fig. 7F1). It is less organic-rich than facies G, based on its color. Examples occur in the Cities Service Ivy #1B and Prairie Marburger #1 cores in Giddings Field (Hayes, 2021).

Facies I: Skeletal wackestone, medium gray, massive. Core of this interval is highly splintered, with horizontal fabric, but without laminations or obvious burrowers (Fig. 7I). This facies occurs in ~5 ft (1.5 m) beds, separated by ~1 ft (0.3 m) beds of unsplintered organic-rich laminated facies. This facies only occurs in the lower portion of the Austin Chalk in well X in Webb County, downdip of the Edwards shelf edge.

Horsetail solution stylolites are common in the more argillaceous chalk intervals, especially in facies E, or at the boundaries between clean chalk and marl beds. Jagged stylolites are rare and only occur in the most carbonate-rich chalk beds. Stylolites indicate that an unknown but probably significant amount of dissolution occurred after deposition.

Interpretation

Austin Chalk facies can be placed in a carbonate ramp profile from updip to downdip (Fig. 8). A carbonate ramp is a gently inclined surface extending from shallow to deep water, with facies bands that parallel the shore, (Ahr, 1973). Sedimentation in the Austin Chalk was dominated by pelagic rainout of phytoplankton and zooplankton, but different facies bands formed due to different amounts of oxygen, light, nutrients, waves, and currents along the depth profile. The ramp formed on a shelf at the edge of the North American continent. Updip facies of the Austin Chalk are interpreted as deposited on the inner ramp (or the inner shelf). Downdip facies are interpreted as deposited on the middle to outer ramp (middle to outer shelf).

Inner ramp facies (facies B and D) are typically light grey skeletal wackestone and packstone, with diverse burrowers and abundant skeletal fragments, interbedded with oyster biostromes (facies C) and thin marl beds. Facies were deposited in the photic zone and fully oxygenated, based on diverse burrows and macrofauna. Depositional environments were subtidal, but were periodically affected by waves, based on channel-forms or scours, widespread oyster beds, and abundant medium to coarse-grained skeletal fragments in outcrop. The shallowest water facies (facies A) occur around the Texas volcanoes, which had ~200 ft (~60 m) of depositional relief (Ewing, 1986). The fringing skeletal packstone and grainstone beds have been interpreted as deposited in different environments and depths, from the beach (Roy et al., 1981; Young, 1985) to gravity fed debrites (Loucks and Reed, 2022). Examples in this study are interpreted as having formed nearly in place due to subregional uplift around volcanoes and were locally redistributed by waves and storms.

Middle ramp facies (facies E) contain medium gray skeletal wackestone with mostly horizontal burrows and disseminated pyrite, interbedded with cyclical marl beds and containing whole inoceramids. The abundant horizontal burrows indicate oxygen was present in the water column but less prevalent in the sediment column.

Outer ramp facies (facies E–H) consist of interbedded medium to dark gray or brown horizontally burrowed or laminated skeletal wackestone, which have greater organic matter, clay, or disseminated pyrite than inner ramp facies. Environments are interpreted as intermittently anaerobic or dysaerobic in the water column and the sediment column, based on the interbedded laminated, organic-rich beds and horizontally burrowed, organic-lean beds. The organic-lean layered facies (facies H) may indicate redistribution of sediment by currents in a downdip dysaerobic setting. The furthest downdip interpreted facies (facies I) is the medium gray splintery facies without obvious burrows or lamination, downdip of the relict Edwards shelf edge. It is interpreted as deposited in an oxygenated environment as an originally soupy sediment that did not preserve burrow traces, possibly modified by gravity flows on a steeper gradient associated with the relict shelf edge.

The upper portion of the Austin Chalk may have been more oxygenated than the lower portion of the Austin Chalk in outer ramp settings. Observations are limited, due to few available cores of this interval, but are based on medium gray colors observed in downdip mudlogs, and core of the uppermost Austin Chalk in the Getty Lloyd Hurt and Shefts Sallie Clark wells, be-

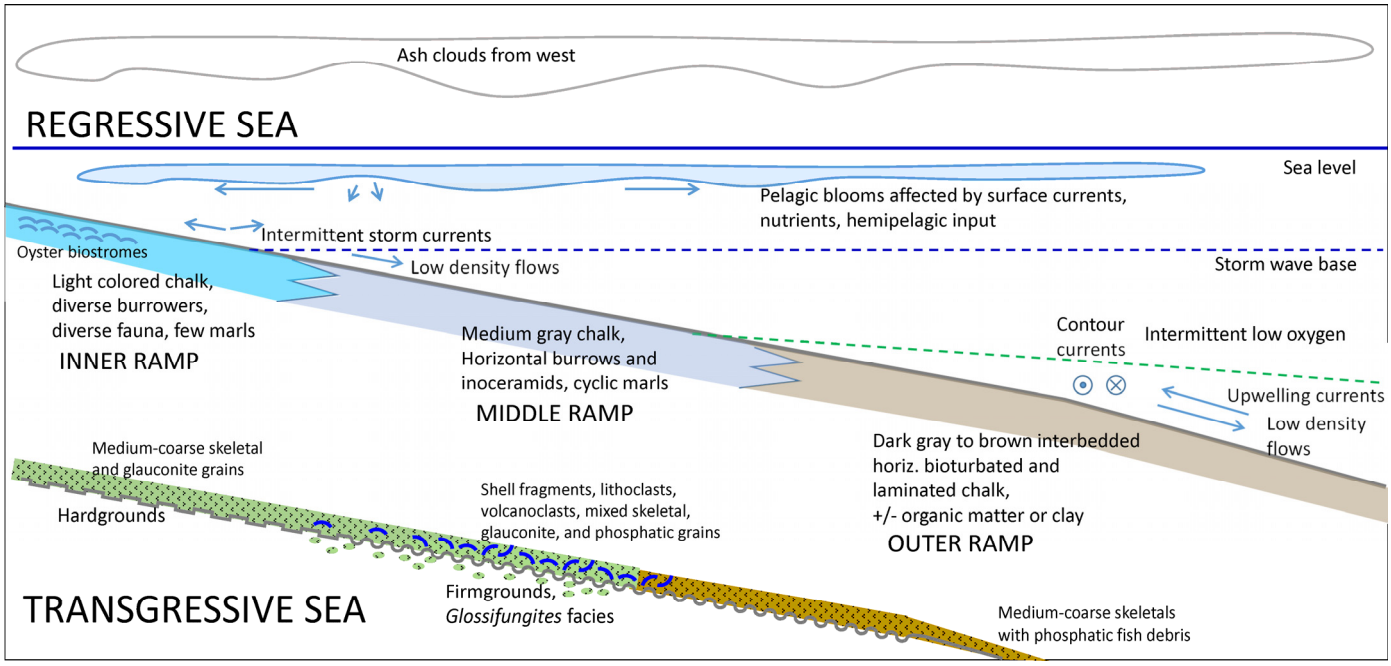

Figure 8. Austin Chalk depositional ramp model. Inner ramp facies are light colored, with more diverse fauna and burrows, becoming darker, less biotically diverse, and more clay- and organic-rich downdip, in intermittently oxygenated outer ramp. Transgressive ramp model shows sequence boundaries, characterized by hardgrounds, firmgrounds, and *Glossifungites* facies, overlain by skeletal and glauconitic grains updip and phosphatic grains downdip.

low the dark gray organic-lean, non-laminated calcareous shales of the Taylor Group.

Facies in Correlation Marker Beds

Cores through the Austin Chalk contain distinctive depositional surfaces or thin beds, which often can be tied to logs and correlated over large distances. Some rock types or facies are specific to updip or downdip settings, and some occur in both (Fig. 9).

Description

Rock type A: Cemented hardgrounds, calcitic or mineralized by iron or phosphatic minerals, often bored and filled by later cement (Fig. 9A). They occur in updip and downdip settings. They are an inch to several inches thick, so may not be recognized in common logs. In some settings, they may be broken into lithoclasts and overlain and surrounded by glauconitic-rich packstone.

Rock type B: Coarse-grained glauconitic skeletal packstone, with poorly sorted skeletal fragments, lithoclasts and intraclasts (Fig. 9B). This facies occurs in updip settings, over the San Marcos Arch and on both flanks. It ranges in thickness from several inches to 11 ft (5 cm to 3.4 m) thick. Macrofossils typically are randomly oriented broken inoceramid fragments, with occasional oysters. Accessary grains include quartz, feldspar, and partially glauconitized volcanic rock fragments. Bored lithoclasts and softer intraclasts are surrounded by burrowed glauconitic skeletal packstone. This facies is widely correlatable, as its increased clay content produces a characteristic medium GR and low resistivity log signature.

Rock type C: Burrows often extend inches to several feet below the main glauconitic zone in a *Glossifungites* ichnofacies (Fig. 9C), recognized by passive fill of open burrows, formed in a firm substrate (Buatois and Mángano, 2011).

Rock type D: Medium to coarse-grained phosphatic skeletal packstone, dominated by fish debris (Fig. 9D). This facies is characteristic of the Eagle Ford Group /Austin Chalk contact,

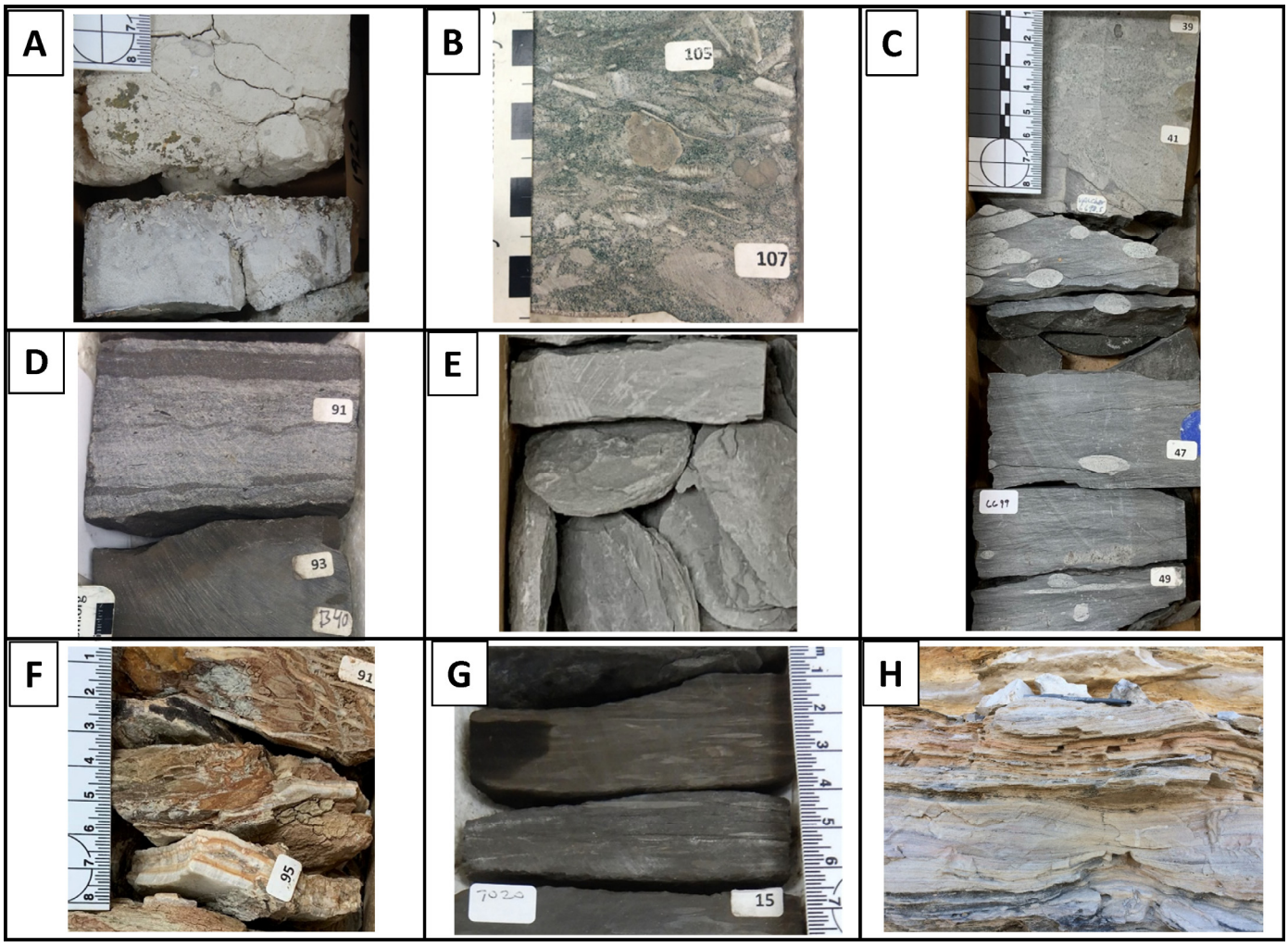

Figure 9. Correlation marker rock types (sequence boundaries and quiet water or flooding surfaces). (A) Mineralized hard ground with borings, Shefts Sallie Clark, 1919 ft (585 m), boundary between Dessau and Pflugerville Fms., AC–III. (B) Glauconitic skeletal packstone with lithoclasts, Getty Lloyd Hurt, 6848 ft (2087 m), Upper Atco Fm., AC–II. (C) *Glossifungites* ichnofacies, firm ground with deep burrowing filled by glauconitic sediment, Tesoro Valcher, 6699 ft (2042 m), Lower Atco Fm., AC–I. (D) Phosphatic lag, Getty Lloyd Hurt, 7217 ft (2200 m), base of the Austin Chalk, AC–I. (E) Calcareous bentonite from a distant volcanic arc, Shefts Sallie Clark, 2100 ft (640 m), Lower Vinson Fm., AC–II. (F) Sutil volcanic tuff, with calcite veins, Tesoro Valcher, 6693 ft (2040 m), within the Lower Atco Fm., AC–I. (G) Dark grey brown horizontally burrowed skeletal wackestone, TOC ~2%, Getty Lloyd Hurt, 7020 ft (2140 m), Lower Atco Fm., 'C' marker, AC–I. (H) Hummocky cross beds in a high uranium zone, US90 outcrop near Langtry, 88 ft (27 m) above the base of the Austin Chalk, Lower Atco Fm., 'D' marker, AC–I.

from the outcrop belt downdip to the submarine plateau. It has admixed glauconitic grains in updip settings, but is mainly phosphatic skeletals downdip.

Rock type E: Bentonite ash beds (Fig. 9E). Bentonite beds generally are calcareous and are bioturbated, based on admixed microfossils and the absence of lamination. They have quartz, feldspar and zircon grains, indicating an acid to intermediate volcanic source. Ash layers typically are 0.5–6 in (1–15 cm), and are characterized by high GR (high thorium on spectral GR) and low resistivity on logs. Thin beds have an outsized effect on resistivity logs, as zones only a few inches thick in core appear to be several feet thick (>1 m) on logs. They are widespread correlation markers across updip and downdip settings.

Rock type F: Ash derived from Texas tuff cones (Fig. 9F) ranges in thickness from several feet to hundreds of feet (1 m to >100 m) thick. The thin edges extend up to ~10 mi (~16 km) laterally. These ashes have low SP, low-medium GR (low thorium), and low resistivity values. The ash was derived from alkaline ultramafic magmas, so consist of altered glass and volcanic fragments, without quartz and feldspar grains. Volcanoes commonly occur in updip settings, stratigraphically within the Austin Chalk or near the Austin Chalk–Taylor contact (Thompson, 2019).

Rock type G: Widespread organic-rich, interbedded laminated and sparsely horizontally burrowed wackestone units (Fig. 9G). This facies is typified by the 'C' and 'D' markers, widely correlative throughout South Texas, due to their unique high GR and high resistivity log signature. Updip in outcrop near Langtry, this facies contains limestone beds having hummocky cross stratification (Fig. 9H).

Interpretation

Widely correlatable thin beds have sequence stratigraphic significance in this study. Hardgrounds and firmgrounds with *Glossifungites* ichnofacies (rock types A and C) are interpreted as forming at sequence boundaries. These are overlain by glauconitic and phosphatic skeletal packstones (rock types B and D), which are interpreted as transgressive lags. These same facies are interpreted as sequence boundaries in the Austin Chalk outcrop between San Antonio and Austin (Cooper et al., 2020; Durham, 1957; Young, 1985). In outcrop, these horizons are regionally correlatable. Where they parallel bedding, they indicate relatively short hiatuses, or higher order sequence boundaries. More significant sequence boundaries in the middle and at the top of the Austin Chalk (Fig. 4) are underlain by angularly truncated beds (Cooper et al., 2020; Durham, 1957; Young, 1985) and have significant nannofossil hiatuses (Jiang, 1989).

Many of the hardgrounds, firmgrounds, and glauconitic skeletal packstone facies in updip cores are regionally correlatable and are tied to the same sequence boundaries recognized by Cooper et al. (2020) in the outcrop and shallow subsurface. Significantly, in the three cores that have nannofossil biostratigraphy (see the next section), glauconitic facies coincide with major biostratigraphic hiatuses, and correlations show angularly truncated sedimentary section beneath the glauconitic facies.

Facies and downdip thinning clinoform geometry (Ewing, 2013) indicate that Austin Chalk deposition occurred over a wide range of water depths, possibly over 1000 ft (>300 m), so the processes that operated at sequence boundaries would have differed along the depth profile. In the inner ramp, waves and storm currents or subaerial exposure would have caused erosion and non-deposition. In the outer ramp, reduced pelagic productivity or contour and upwelling currents would have caused condensed section due to non-deposition and erosion.

Hardgrounds and firmgrounds are interpreted to form on the inner and outer ramp during sediment hiatuses. In the inner ramp, light colored chalk hardgrounds and firmgrounds would have formed and broken into lithoclasts or intraclasts when exposed to storms, burrowers and borers, or subaerial processes. Hardgrounds also would have formed (and remained intact) on the outer ramp in condensed intervals, where sequence boundaries and maximum flooding surfaces converge (for example, the dark gray hardground at the base of the Austin Chalk in well Y in Karnes County and the medium grey hardground near the top of the Austin Chalk in the Shefts Sallie Clark core).

As sea level rose over the ramp, a transgressive glauconitic and phosphatic lag would have covered the hardened surface and filled the open burrows and borings, forming a *Glossifungites* ichnofacies, characteristic of transgressive environments (Buatois and Mángano, 2011). Burrows filled by glauconite reach several inches to several feet (5–60 cm) below the hardened surfaces in Austin Chalk cores (Tesoro Valcher and Shefts Sallie Clark wells) and in outcrops (Cooper et al., 2020). Due to long hiatuses, transgressive facies amalgamate grains from different sources, including bentonites and Texas volcanic tuffs. Transgressive facies change from glauconitic-rich packstone to mainly phosphatic skeletal packstone downdip (Fig. 8). Inch thick (cm) beds of phosphatic-rich packstone occur at the Eagle Ford Group / Austin Chalk sequence boundary, even downdip of the Edwards shelf margin, on the submarine plateau (in well X). Thus, transgression over a sequence boundary can be recognized even in deep water settings, likely due to more energetic bottom currents.

Ash beds (rock type E) are widely correlatable and interpreted as deposited in quiet water, between sequence boundaries. Their composition (containing quartz and feldspar grains) and areal extent (covering hundreds of square miles) indicate that they were derived from distant western volcanic arcs (Hovorka, 1998; Lee et al., 2018). Ash falls are not dependent on sea level fluctuations, but some of the thickest, most widespread bentonite beds have different GR and SP character above and below the ash, so they are interpreted as being deposited near maximum flooding surfaces. The thin ash layers (rock type F) that extend for several miles around Texas tuff cones were deposited by subaerial fallout, and redistributed by waves and slope failure. Their preservation indicates deposition in relatively quiet water between sequence boundaries.

The 'C' and 'D' organic-rich markers (rock type G) are unique to the Maverick Basin in South Texas. They are interpreted as maximum flooding surfaces, since low oxygen and organic matter preservation are more common in deeper water settings of the Austin Chalk. However, in South Texas, these markers were deposited across a wide range of paleowater depths, based on sigmoidal depositional geometry, downdip downlap, updip pinch out, and hummocky cross bedding in the Langtry outcrop (Griffith et al., 2019). These markers are interpreted as deposited in a widespread oxygen minimum zone that extended into shallower water depths, due to unique oceanographic conditions, like those during deposition of the Lower Eagle Ford Formation.

Biostratigraphy, Correlations, and Sequence Stratigraphy

The nannofossil biostratigraphic scheme in this study (Fig. 10) is a modification of the standard Sissingh (1977) zonation with additions taken from Bralower and Bergen (1998) and Bergen and Sikora (1999). The chart shows the tie between the nannofossils, Cretaceous stage names, and the 2012 global time scale (Ogg and Hinnov, 2012) used in this study. It incorporates nannofossil biostratigraphic concepts from Jiang (1989) from the type sections of the Austin Chalk formations near Austin (Fig. 5).

Three nannofossils have particular importance in the wells studied. The LO of *Micula decussata* is used to mark the boundary between the early and middle Coniacian (between CC13 and CC14). The highest occurrence (HO) of *Lithastrinus septenarius* is used to denote the early/middle Santonian boundary (within the combined CC15–16 zone). The LO of *Ahmuellerella regularis* is used similarly to Jiang (1989) to approximate the bounda-

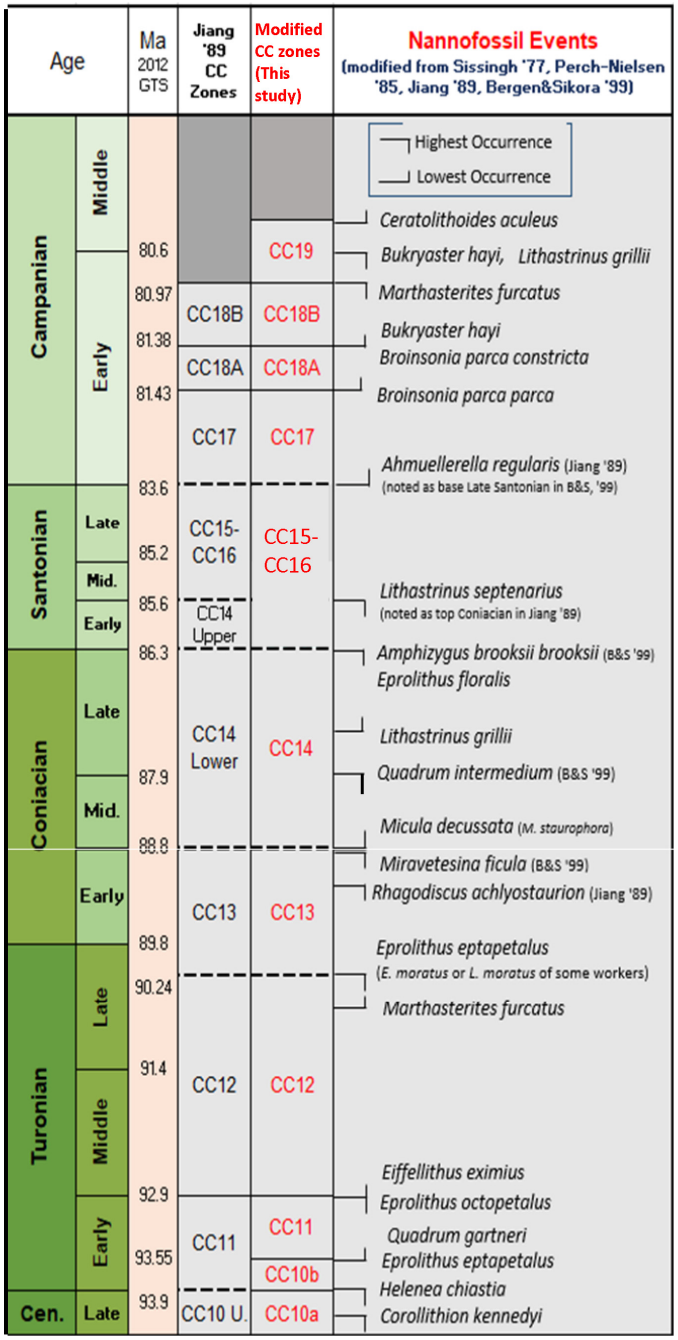

Figure 10. Nannofossil biostratigraphic chart. Chart is from J. Pospichal (modified after Bergen and Sikora [1999]; Jiang [1989]; Perch-Nielsen [1985]; and Sissingh [1977]. Age dates are Ogg and Hinnov (2012).

ry between the late Santonian and early Campanian (between CC16 and CC17).

Nannofossil samples in this study are from two cores on either side of the San Marcos Arch and one core on the San Marcos Arch. Significant biostratigraphic hiatuses coincide with glauconitic intervals; these were the main criteria used to recognize sequence boundaries and correlate away from these three wells. Correlations were also based on ties to the lithostratigraphy and biostratigraphy in outcrop. Additional biostratigraphy would be useful to further constrain the Austin Chalk sequences in areas away from the data in this study.

Getty Lloyd Hurt

The core in the Getty Lloyd Hurt #1 well (4228330305, TD 7239 ft (2206 m), La Salle County) (Fig. 11) was proposed as the type core for the Austin Chalk in South Texas (Loucks et al., 2020b) and is excellent example of the varied facies in the Austin Chalk. The well is in Pearsall Field, downplunge on the Pearsall Arch, and west of the San Marcos Arch. The full core covers an interval of 573 ft (175 m), from 6731–7304 ft (2052–2226 m). The Austin Chalk portion is 473 ft (144 m), from 6745–7218 ft (2056–2200 m). The core includes 15 ft (4.6 m) of calcareous shale and argillaceous marl of the lower Anacacho Formation and 87 ft (26.5 m) of the underlying Upper Eagle Ford Formation. The Austin Chalk portion of the core has one large and multiple small labeled gaps. No systematic core shift was noted, but detailed ties between log and core have an uncertainty of up to 5 ft (1.5 m), due to frequent discrepancies between labeled intervals and actual core footage in the core boxes. These small gaps are not represented in the core description to avoid a choppy display.

The Austin Chalk has a phosphatic lag at its base, and interbedded laminated and horizontally burrowed organic-rich chalk in the 'C' through 'E' units (Pearsall Field stratigraphy from Ewing [2013]). The lithology changes upward to a medium gray chalk with mainly horizontal burrows and then diverse burrows in the upper 'B–2 unit,' which is overlain by the 'B–1' interval with multiple glauconitic packstone beds. The 'B–1' interval is overlain by light-colored, diversely burrowed chalk in the lower 'A' unit. The upper part of the 'A' unit is darker gray and argillaceous with mainly horizontal burrows and is overlain by dark gray calcareous shale at the base of the Anacacho Formation.

XRF data indicates that the highest percent Ca is near the base of the Austin Chalk and the top of 'B–2' unit. The upper 'A' and 'B–1' units have more clay, based on increased Si, Al, and K. The organic-rich facies in units 'C' through 'E' have increased Ni, V, and Sr. The glauconite beds in the 'B–1' unit are recognized by peaks in K, Fe, and P. Mn is enriched at the top of the 'B–2' unit, directly below the basal glauconite bed in the 'B–1' unit.

Twenty-seven biostratigraphic samples were analyzed in the Getty Lloyd Hurt well, 23 of which were in the Austin Chalk (Appendix B in Griffith [2023]). Nannofossils are common to abundant throughout the section and preservation varies from poor to moderate. Higher abundances are noted at the top and bottom of the section.

A slight depth shift is necessary at the base of the Austin Chalk to resolve the log-core discrepancy. The log base of the Austin Chalk is at 7212 ft (2198 m). The base of the Austin Chalk in core is recognized by multiple phosphatic skeletal lag beds, from 1/2 inch to several inches thick (1–10 cm) from ~7214 to 7218 ft (2199–2200 m). The nannofossil sample at ~7215 ft (2199 m) within the basal Austin Chalk has LO *Lithastrinus septenarius*, indicating an age no older than late Turonian CC12–13. The interval from the base of the Austin Chalk to the top of the 'B–2' zone, from 6860–7212 ft (2091–2198 m) is 352 ft (107 m) thick, and it is entirely upper Turonian–lower Coniacian CC13. There are no biostratigraphic breaks at the 'C' and 'D' organic-rich markers.

The LO *Micula decussata* (base middle-late Coniacian CC14) occurs at 6858.7 ft (2121 m), near the base of the 'B–1' unit at 6860 ft (2091 m), within a glauconitic skeletal packstone covering 6858–6859.5 ft (2090.2–2090.7 m). Traces of glauconite extend below this layer down to 6863 ft (2091.4 m). A hiatus occurs at the boundary between the 'B–2' and 'B–1' zones, with much of the middle and late Coniacian is missing.

The log boundary between the 'B–1' and 'A' zones occurs at 6802 ft (2073 m). The underlying biostratigraphic sample in the upper 'B–1' zone at 6813.3 (2076.5 m) contains the HO *Lithastrinus septenarius* and the HO *Eprolithus floralis*, indicat-

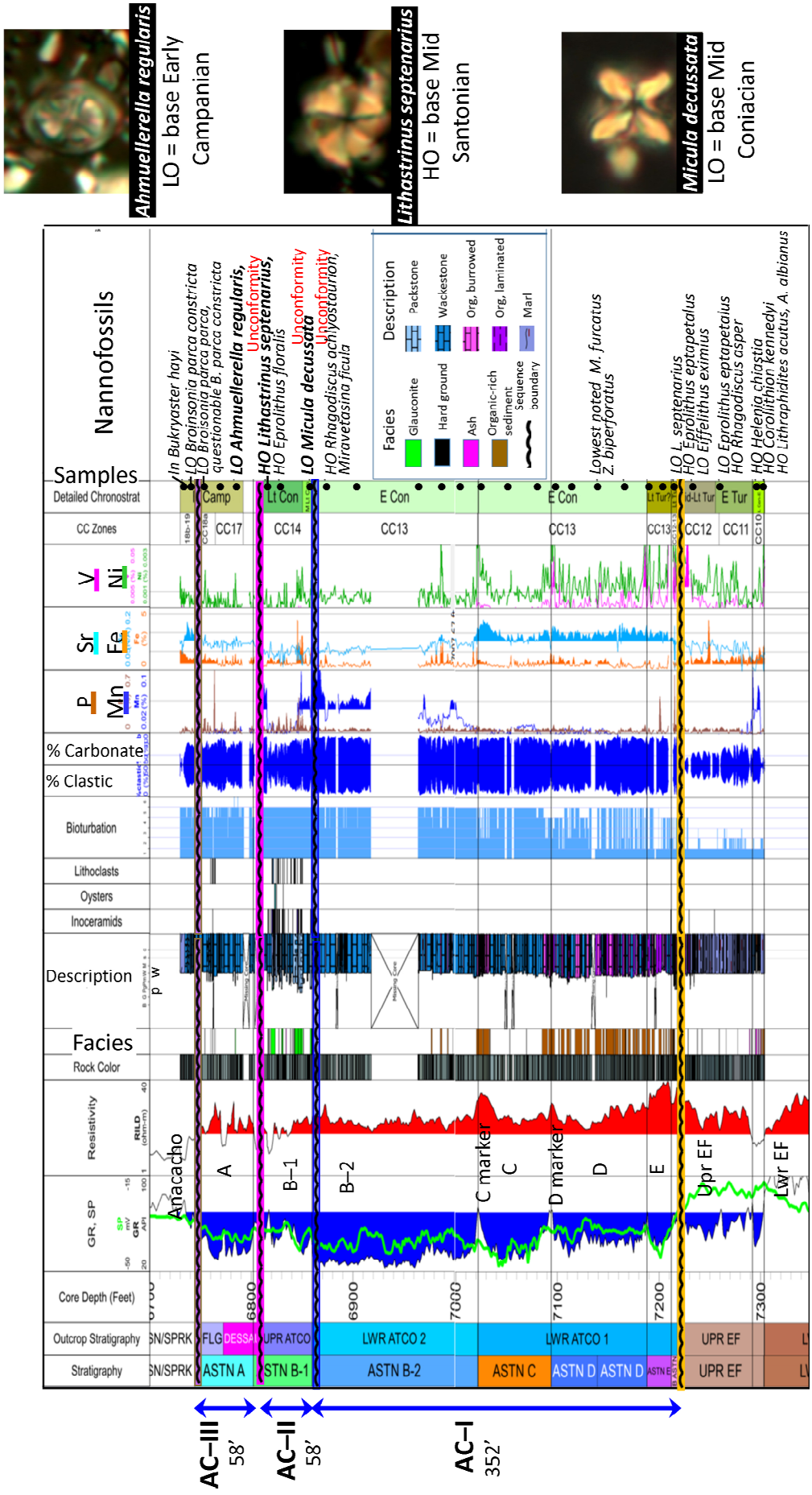

Figure 11. Well log, facies, XRF data, and key nannofossils in the Getty Lloyd Hurt #1. Nannofossil analysis is by James Pospichal. Stratigraphy is from Pearsall Field (Ewing 2013). The lower portion of the Austin Chalk consists of interbedded laminated to horizontally burrowed wackestone. Chalk has a brownish hue in beds with higher organic content (brown in facies column). Colors are lighter and bioturbation increases upward in the Austin Chalk. Glauconitic skeletal packstone beds (green in facies column) in ‘B–1’ interval coincide with biostratigraphic hiatuses. Images show key nannofossils highlighted in bold text on chart. Key fossils occur in ‘B–1’ and ‘A’ intervals.

ing this sample is late Coniacian CC14. The overlying sample, in the lower 'A' zone, at 6784.3 ft (2068 m) has the LO *Ahmuellerella regularis* (early Campanian, CC17). The thin interval between these two samples indicates a long hiatus, with the Santonian missing. The Getty Lloyd Hurt core does not contain a glauconitic packstone bed between these two samples, but a 7 ft (2.1 m) core gap exists from 6803–6810 ft (2073.5–2075.6 m). A thin, thorium-rich ash can be correlated into the core gap, based on spectral GR in the Enercorp Rally 1–H well (4216332960), 8 mi (13 km) away (Ewing, 2013). Correlations and descriptions of the upper 'B–1' interval in two nearby cores, the Proco Gise #1 (4212732878) and Champlin Rogers #1014 (4212731164), 6 and 11 mi (10 and 18 km) away, respectively (Loucks and Reed, 2022; Zheng et al., 2021) indicate that a glauconitic packstone may occur in this core gap.

The log top of the Austin Chalk is at 6744 ft (2055.5 m). The underlying sample in the upper 'A' interval, at 6749.5 ft (2057 m) has LO *Broinsonia parca parca* (early Campanian CC18a). The sample at 6738.5 (2054 m) from just above the top of the Austin Chalk has LO *Broinsonia parca constricta* (early Campanian CC18b). The uppermost sample at 6735.5 ft (2054 m) in the shale at the base of the Anacacho Formation has LO of *Bukryaster hayi* (early Campanian CC18b–CC19).

Facies interpretations of the Getty Lloyd Hurt indicate that there are at least two major sequences in the Austin Chalk that can be sub-divided into smaller depositional sequences. The sequence stratigraphic model is based on two main ideas: lighter colored, thoroughly bioturbated chalk is associated with higher oxygen and shallower water, and sequences are separated by transgressive lags. The lower Austin Chalk sequence starts with a transgressive lag at the Eagle Ford–Austin Chalk sequence boundary, followed by a long regression through the top of the diversely burrowed 'B–2' interval. The lower portion of the Austin Chalk (units 'C,' 'D,' and 'E') was deposited in an outer ramp setting having intermittent low oxygen. The widespread organic-rich 'C' and 'D' markers are interpreted as maximum flooding surfaces, associated with higher order sequences. Water depths gradually shallowed to an inner ramp setting in the 'B–2' interval of the Austin Chalk. The basal skeletal- and intraclast-rich glauconite bed in the 'B–1' interval is interpreted as a transgressive lag overlying a sequence boundary. This interpretation based on: outcrop analogs (e.g., Cooper et al., 2020; Durham, 1957), a hiatus as indicated by nannofossils, ties to other cores and mudlogs with glauconitic-rich beds in 'B–1' interval in the Pearsall area (Loucks and Reed, 2022; Zheng et al., 2021), and correlations showing great thickening of the 'B–2' interval to the west (Durham and Hall, 1991; Ewing, 2013). Correlations in this study (Griffith, 2023) indicate angular truncation of a thick 'B–2' interval below the 'B–1' interval. The multiple glauconite-rich lags in the 'B–1' interval in the Getty Lloyd Hurt well indicate additional sea level fluctuations and sequence boundaries not traceable in correlations or biostratigraphy. The highly bioturbated 'A' interval records a regression followed by transgression near the top of the Austin Chalk, below the basal calcareous shale of the Anacacho Formation.

Nannofossil biostratigraphy provides additional detail about the stratigraphic sequences in the Getty Lloyd Hurt. Biostratigraphy indicates that the Austin Chalk consists of three main stratigraphic sequences, separated by two large hiatuses (Fig. 11). The lowest Austin Chalk biostratigraphic sequence, from 'E' through the 'B–2' interval is called AC–I in this study. It has 352 ft (107 m) of upper Turonian–lower Coniacian CC13 section that covers ~1.5 My. The second Austin Chalk sequence, AC–II, includes most of the 'B–1' interval and is upper Coniacian CC14. The third Austin Chalk sequence, AC–III is lower Campanian CC17–18 and includes the uppermost 'B–1' and 'A' intervals. A major hiatus separates the lower Coniacian AC–I and upper Coniacian AC–II sequences, at the base of the glauconitic-rich 'B–1' unit. A second major hiatus separates the upper Coniacian AC–II and lower Campanian AC–III strata (with the Santonian CC15–16 missing), near the top of the 'B–1' unit. The AC–II sequence is only 58 ft (17.7 m) thick, but represents roughly 5 My.

Stratigraphic nomenclature in Pearsall Field can be tied to the Austin Chalk lithostratigraphic formations in outcrop from San Antonio to Austin (Cooper et al., 2020; Durham, 1957), based on biostratigraphic ties to global time scale (Jiang, 1989; Young, 1985) and log and outcrop correlations. AC–I is equivalent to the Lower Atco Formation, AC–II is equivalent to the Upper Atco Formation, and AC–III is equivalent to the upper Dessau and Pflugerville formations. The Santonian-age Vinson and Jonah formations are missing in the Getty Lloyd Hurt well.

Tesoro Valcher

The Tesoro Valcher #1 (4249330230, TD 7008 ft (2136 m), Wilson County) is on the San Marcos Arch, 72 miles (116 km) east of the Getty Lloyd Hurt core (Fig. 12). The 144 ft (44 m) thick core, from 6660–6804 ft (2030–2074 m), is a partial penetration of the Austin Chalk. The base of the core is just above the Eagle Ford / Austin Chalk contact. The top of the core is about 40 ft (12.2 m) below the top of the Austin Chalk (the contact with the Anacacho Formation is difficult to pick in this area, due to similar lithology). The core is in good shape, with few missing intervals. No shift was applied, and intervals in boxes match well with labels.

Stratigraphic markers from Pearsall Field can be correlated into the Tesoro Valcher well, although intervals are much thinner than the Getty Lloyd Hurt. The 'D' interval is a medium grey chalk with horizontal burrows without any organic-rich or laminated facies. The widespread 'C' and 'D' markers in Pearsall Field merge and pinch out 3 mi (5 km) southwest of the Tesoro Valcher well but the extended correlation coincides with two glauconitic zones at 6696 ft and 6698 ft (2040.8 and 2041.5 m) in the Tesoro Valcher well. *Glossifungites* facies extend 1 ft (30 cm) below the lower glauconitic zone. The upper glauconitic zone is 5 ft (1.5 m) below the base of a prominent ash bed, with medium-low GR, low SP and low resistivity log character. The ash can be correlated to the small Upper Cretaceous Sutil tuff volcano (Ewing, 1986), 2 mi (3 km) toward the northeast. The 4 ft (1.2 m) thick ash bed is overlain by an 11 ft (3.4 m) thick coarse skeletal packstone, dominated by red algae, (described by Loucks and Reed [2022]) that has low GR, pronounced negative SP, and medium resistivity log character. Maps indicate that this skeletal packstone surrounds the several hundred foot (~60 m) high Sutil tuff cone, but it is best developed on the west side of the cone above a much thinner ash layer (Ewing, 1986; Matthews, 1986). The skeletal packstone is overlain by several glauconitic-rich beds and a medium gray diverse burrowed chalk interval in the 'B–1' unit at the top of the core. The 'A' unit was not cored.

Nineteen biostratigraphic samples were analyzed for nannofossils in the Tesoro Valcher well (Appendix B in Griffith [2023]). Nannofossil abundance is high at the top of the core and moderate to low in other intervals. Nannofossil preservation is poor to fair throughout the core.

The base of the Tesoro Valcher core is at 6804 ft (2073.8 m), about 1 ft (0.3 m) above the log pick for the base Austin Chalk. The 124 ft (38 m) thick interval from 6679–6803 ft (2035.7–2073.5 m) has early Coniacian CC13 nannofossils. The sample within the 4 ft (1.2 m) thick ash at 6693 ft (2040 m) yielded early Coniacian CC13 nannofossils, whereas the overlying sample at 6688.75 (2038.6 m) within the 11 ft (3.4 m) thick coarse skeletal packstone was barren.

The next sample at 6679 ft (2035.7 m) is from the base of an 8 ft (2.4 m) thick glauconitic skeletal packstone that extends from 6672–6680 ft (2033.5–2036 m). It has LO *Micula decussata* and other nannofossils of latest late Coniacian CC14. A hiatus, covering the middle Coniacian and much of the upper Coniacian, oc-

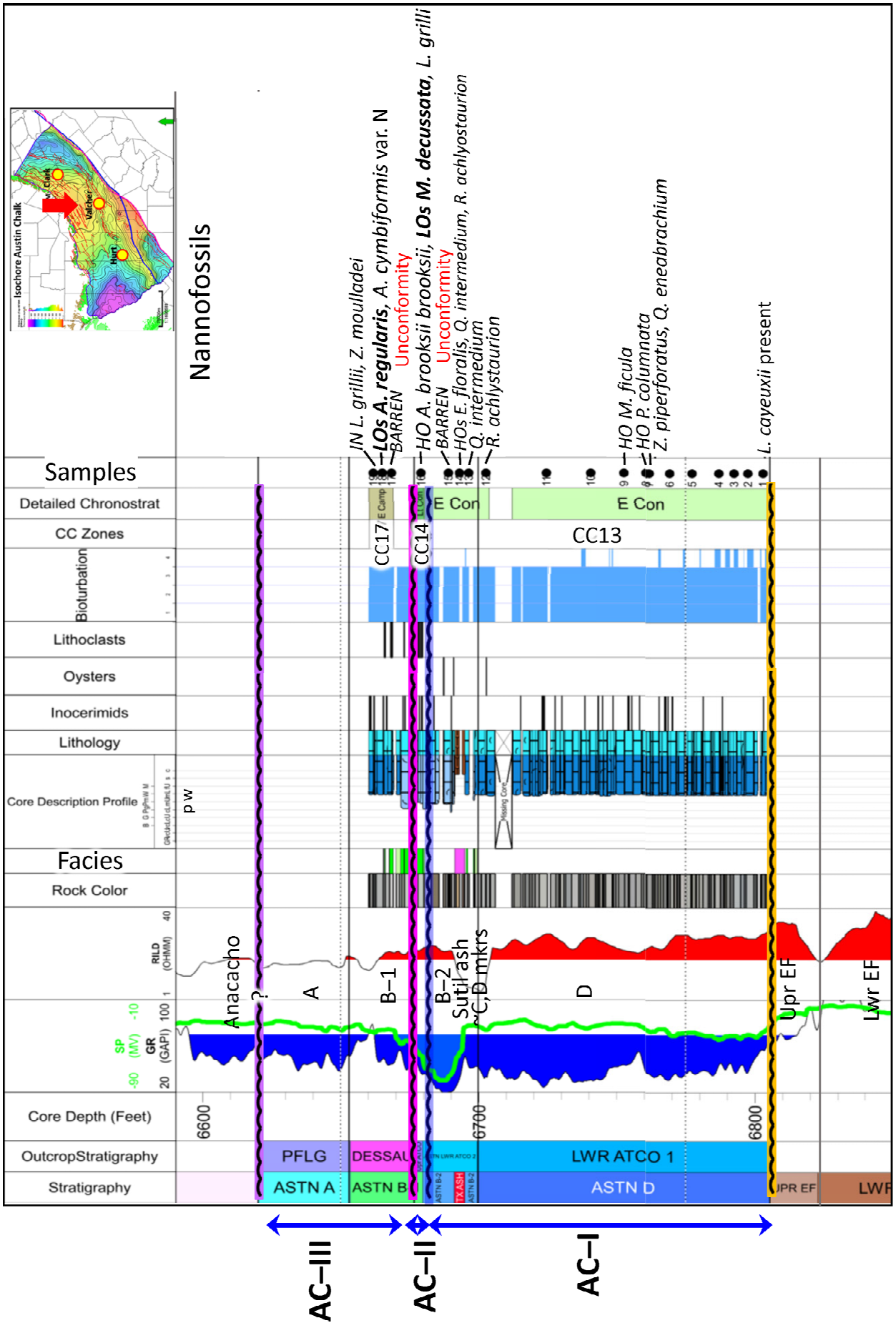

Figure 12. Well log, facies, and key nannofossils in the Tesoro Valcher #1. Nannofossil analysis is by Eric de Kaenel. Stratigraphy is from Pearsall Field (Ewing, 2013). The lower Austin Chalk consists of horizontally burrowed wackestone. Thin glauconitic facies and *Glossifungites* ichnofacies occur at the correlated position of eroded 'C' and 'D' markers. Ash from Sutil volcano is overlain by coarse skeletal packstone, in interval correlated to 'B–2'. Glauconitic skeletal packstone beds (green in facies column), biostratigraphic hiatuses, and key fossils occur in 'B–1' interval.

curs between 6679 ft and 6693 ft (2035.7 and 2040 m) samples. The overlying sample at 6665 ft (2034.4 m) is from a light-colored well-burrowed wackestone above a 2.5 ft (0.8 m) thick glauconitic skeletal packstone from 6667.5 to 6669 ft (2032.2–2032.6 m) containing large bored lithoclasts. This sample contains LO *Ahmuellerella regularis* of early Campanian CC17, indicating another large hiatus, covering the entire Santonian, between the 6665 ft and 6679 ft (2034.4 m and 2035.7 m) samples.

The facies in the lower Austin Chalk ('D' interval) are interpreted as deposited on a middle ramp with moderate oxygen levels, depositionally updip from the Getty Lloyd Hurt well. The 'C and 'D' markers are interpreted as eroded, based on the glauconitic-rich lag and *Glossifungites* ichnofacies at their equivalent positions. The red algal skeletal packstone facies overlying the local ash bed is interpreted as a shallower water deposit, formed nearly in place by structural uplift, rather than shed from the relatively small Sutil volcano, based on its composition and wide areal extent. The 'B–2' interval under 'B–1' thins dramatically eastward from Getty Lloyd, and is interpreted as truncated by erosion; the 'B–1' is interpreted as a transgressive glauconitic lag.

Nannofossil biostratigraphy in the Tesoro Valcher indicates three main sequences in the Austin Chalk, separated by two hiatuses. The lowest sequence, AC–I, 128 ft (39 m) from the 'D' through 'B–2' interval, is upper Turonian-lower Coniacian CC13. The second sequence, AC–II, is ~5 ft (1.5 m) and represented by a single sample at the base of the 'B–1' interval having late Coniacian CC14 nannofossils. The third sequence, AC–III, includes the upper 'B–1' interval and is lower Campanian CC17. Two hiatuses occur on either side of the AC–II sequence. The lower hiatus, where the middle Coniacian is missing, occurs at the base of the glauconitic-rich 'B–1' unit. The upper hiatus, where much of the upper Coniacian and Santonian is missing, occurs within the 'B–1' unit. The very thin AC-II sequence represents more than 5 My. The 'A' interval and Anacacho Formation were not cored, so do not give any data on this contact, but the chalk on chalk contact and thinning of Anacacho interval indicate a likely hiatus, like in San Antonio (Cooper et al, 2020; Jiang, 1989).

Based on nannofossil biostratigraphy and correlations, the AC–I sequence is equivalent to the lower Atco, the very thin AC–II is Upper Atco Formation, and AC–III is equivalent to the upper Dessau and younger formations. The Vinson and Jonah formations are missing in this well.

Shefts Sallie Clark

The Shefts Sallie Clark #1 (4205501852, TD 2221 ft (677 m), Caldwell County, has a 333 ft (101.5 m) core with a complete penetration of the Austin Chalk (Fig. 13). The well was drilled on the east side of the San Marcos Arch, 66 mi (107 km) northeast of the Tesoro Valcher well, in the Luling-Branyon Field, on the upthrown side of a large counter-regional fault. The Austin Chalk section is 280 ft (85 m), from 1892 to 2172 ft (577–662 m). The core includes a 16 ft (5 m) penetration of the lower Taylor Sprinkle Formation from 1876 to 1892 ft (572–577 m), 17 ft (5 m) of the Eagle Ford and Pepper formations from 2172 to 2189 ft (662–667.2 m), and 21 ft (6.4 m) of Buda Limestone from 2189 to 2210 ft (667.2–673.6 m). No shift was applied, and intervals in boxes match well with labels.

Pearsall nomenclature cannot be used on the east side of the San Marcos Arch. Although the glauconite-rich 'B–1' interval can be correlated, the 'C' and 'D' markers pinch out and are not recognized east of the arch. The facies in the Shefts Sallie Clark well are described using outcrop lithostratigraphy correlated into the shallow subsurface (Cooper et al., 2020) and tying the nannofossil biostratigraphy in the well and type sections in outcrop (Jiang, 1989) (Figs. 5 and 10).

The Eagle Ford Group in the Shefts Sallie Clark well has three very thin but distinct units: 5 ft (1.5 m) non-calcareous Pepper Shale, 9 ft (2.7 m) organic-rich Lower Eagle Ford Formation, and 3 ft (1 m) medium-gray argillaceous burrowed Upper Eagle Ford Formation. A hardground occurs at the base of the Austin Chalk, underlain by a *Glossifungites* facies, with coarse glauconitic sediment extending in large burrows 1 ft (0.3 m) into the Upper Eagle Ford Formation. The basal hardground is overlain by a phosphatic lag. The lowest 8 ft (2.8 m) of Austin Chalk is medium-light gray and diversely burrowed wackestone and is overlain by an 11 ft (3.4 m) glauconitic skeletal packstone.

Overlying the glauconitic facies is 161 ft (49 m) light gray and diversely burrowed Austin Chalk, from 1992 ft to 2153 ft (398–431 m), with occasional interbeds of ash, marl, and oyster packstone. The overlying 74 ft (22.6 m) of the Austin Chalk, from 1918 ft to 1992 ft 384–398 m) is similar but contains several 2–5 ft (0.6–1.5 m) glauconitic skeletal packstone beds. The uppermost portion of the Austin Chalk (24 ft [7 m]), from 1894–1918 ft (379–384 m) is medium gray, more argillaceous, with mainly horizontal burrows.

XRF data shows a high percent Ca in clean chalk intervals compared to marl and ash beds, increased Si, Al, K P, and Fe in glauconitic zones, and Mn enrichment below glauconite beds. Si, Al, Fe, and Sr increase in the upper portion of the Austin Chalk, indicating higher argillaceous content (McCreary, 2022).

Twenty-one nannofossil samples were analyzed in Shefts Sallie Clark well (14 from the Austin Chalk interval) (Appendix B in Griffith [2023]). Nannofossil abundance and preservation are moderate at the base, poor in the middle, and good at the top of the Austin Chalk. Some contamination with drilling mud was noted in the lower part of the core.

The biostratigraphy from this well is very different from the previous two wells. The lower Coniacian CC13 is extremely thin, and a thick upper Coniacian–Santonian CC14–CC16 section occurs in this well that is not present in the other two wells.

The sample at 2172 ft (662 m), from just below the hardground at the Austin Chalk–Upper Eagle Ford contact, has nannofossils indicating upper Turonian–lower Coniacian CC13. The overlying sample, at 2161.5 ft (658.8 m), 10 ft (3 m) above the base of the Austin Chalk, is just above the base of an 11 ft (3.4 m) fossiliferous glauconitic lag from 2153–2164 ft (656.2–659.6 m). It has HO *Eprolithus floralis*, LO *Lithastrinus grillii* and a few *Micula decussata*, indicating middle-late Coniacian CC14. The overlying sample at 2139 ft (652 m), above the glauconitic zone, has frequent *M. decussata* and is correlated to the Upper Atco Formation.

The overlying sample at 2112 ft (643.7 m), 60 ft (18.3 m) above the base of the Austin Chalk, has the HO *Lithastrinus septenarius* characteristic of the base middle Santonian, within CC15–16 zone, and is correlated to the Vinson Formation. The samples from 1961.7–2112 ft (598–643.7 m) have nannofossils characteristic of middle-upper Santonian CC15–16.

The sample at 1940.8 ft (591.5 m) is from an oyster-rich interval and has LO of *Ahmuellerella regularis* of early Campanian CC17. This sample is 16 ft above the glauconitic packstone beds 1957–1963 ft (596.5–598.3 m), interpreted to be at the base Dessau Formation. A hardground at 1916 ft (584 m) marks the boundary between the Dessau and Pflugerville Formations, based on samples at 1919.5 ft (585 m) and 1900 ft (597 m), of early Campanian CC17 and CC18a age . The shallowest sample, from 1876 ft (571.8 m), is from the Sprinkle Formation, 18 ft (5.5 m) above top of the Austin Chalk and has nannofossils from early Campanian CC18b.

Facies in the Shefts Sallie Clark well are interpreted to be mostly deposited on the inner ramp, at a shallower water depth than the facies in the other two wells, based on color, diverse burrowing, and multiple oyster biostromes. Glauconitic skeletal packstone beds are interpreted to be transgressive lags on top of sequence boundaries. The argillaceous, horizontally burrowed

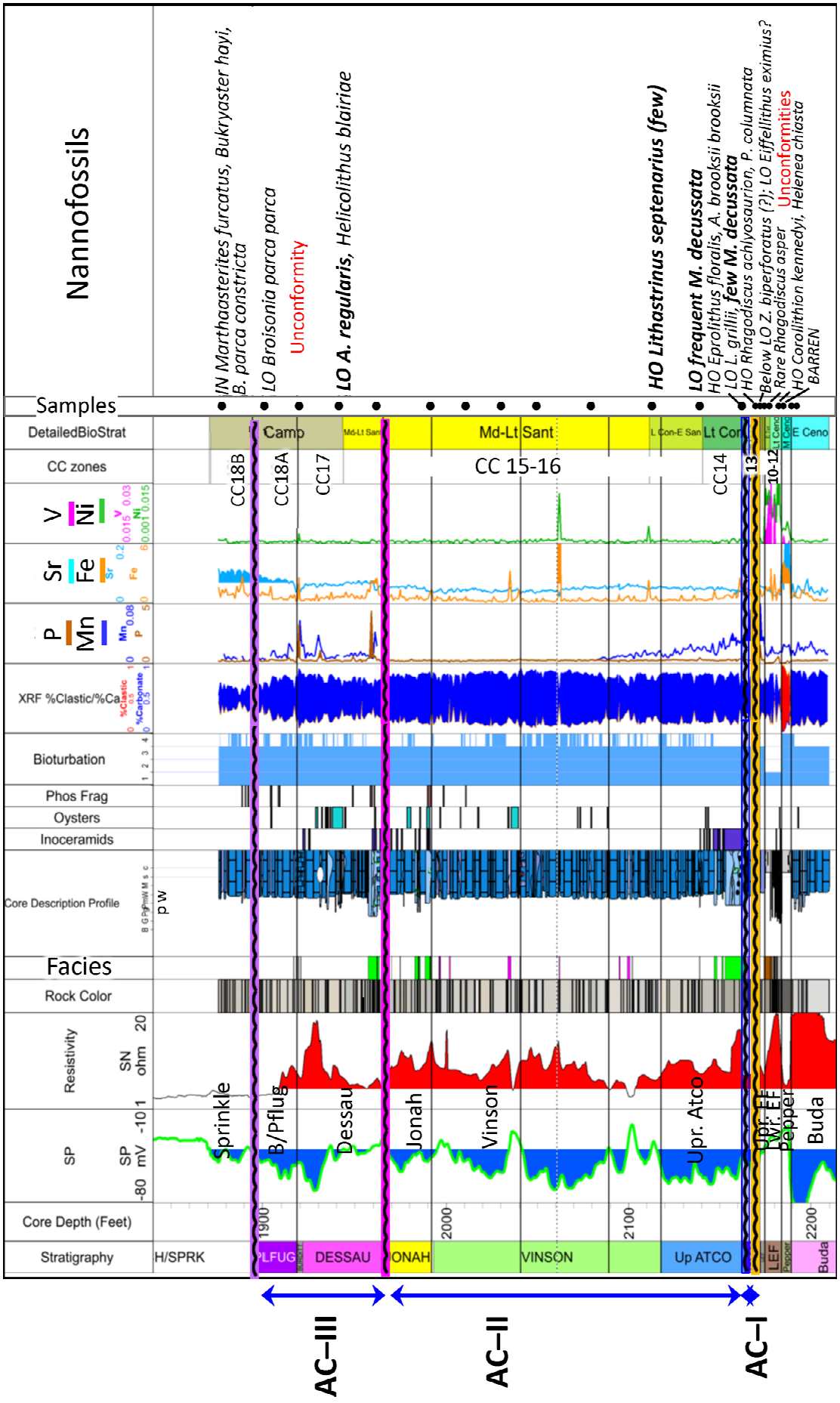

Figure 13. Well log, facies, XRF data, and key nannofossils in the Shefts Sallie Clark #1. Nannofossil analysis is by James Pospichal. Stratigraphy is from outcrop and shallow subsurface (Cooper et. al., 2020; Jiang, 1989). Austin Chalk is light colored and diversely burrowed, with interbedded oyster beds and thin marls and ashes. Glauconitic skeletal packstone beds (green in facies column) occur near the base of the Austin Chalk in the Atco Formation, and near the bases of the Jonah and Dessau formations. Key fossils occur across the interval from the Atco to Dessau formations.

unit near the top of Austin Chalk (Pflugerville Formation) is interpreted as deposited in deeper water than the rest of the section.

Three sequences occur in the Shefts Sallie Clark well, like in the other two wells, separated by two hiatuses. The lowest biostratigraphic sequence, AC–I, is represented by only 8 ft (2.4 m) of lower Coniacian CC13, at the base of the Austin Chalk Group (equivalent to Lower Atco Formation). The second sequence, AC–II, is a 200 ft (60 m) thick interval between the lower and upper glauconitic beds that has upper Coniacian to upper Santonian CC14 and CC15–16 nannofossils (equivalent to the Upper Atco, Vinson, and Jonah formations). This interval is mostly missing in the other two wells. The third sequence, AC–III, is a 95 ft (29 m) thick interval containing upper Santonian-lower Campanian (upper CC15–16 to CC18) nannofossils. Sequence AC–II is bounded by two hiatuses. The lower hiatus, near the base of the Austin Chalk, indicates missing middle-upper Coniacian section. The upper hiatus, at the base of the Dessau Formation, is within the upper Santonian.

Three Well Cross Section

A cross section of the three wells with new nannofossil biostratigraphy (Fig. 14) shows the striking asymmetry of the Austin Chalk sequences across the San Marcos Arch. The LO of *Micula decussata* of middle-late Coniacian CC14 is in the upper portion of the Austin Chalk in the Getty Lloyd Hurt and Tesoro Valcher cores, but in the basal portion of the Austin Chalk in the Shefts Sallie Clark core. The LO of *Ahmuellerella regularis* of early Campanian CC17 is in the upper portion of the Austin Chalk in all three wells (datum for the cross section). The HO of *Lithastrinus septenarius* is directly below the LO of *A. regularis* in the Getty Lloyd Hurt well but is separated by 171 ft (52 m) of middle-upper Santonian CC15–16 in the Shefts Sallie Clark well.

Based on these three fossils, the three unconformity-bound stratigraphic sequences in the Austin Chalk are delineated. The sequence boundaries are based on biostratigraphic hiatuses and coincide with glauconitic horizons. The three sequences are composite sequences; each contains several higher order sequences that can be tied to the lithostratigraphic formations in outcrop (Atco through Pflugerville formations). The first sequence, AC–I (upper Turonian to middle Coniacian Lower Atco Formation) is best developed in the Getty Lloyd Hurt well and is unconformably overlain by AC–II (upper Coniacian) chalk. The second sequence, AC–II (upper Coniacian to Santonian Upper Atco to Jonah formations) is best developed in the Shefts Sallie Clark well and is unconformably overlain by the third sequence, AC–III (upper Santonian–lower Campanian Dessau and Pflugerville).

The large thickness differences in the first two sedimentary sequences in this strike section are interpreted as due to differences in subsidence and uplift, based on facies and correlations (Fig. 15). During deposition of sequence AC–I, greater subsidence occurred in the west, as erosion and uplift occurred in the east. During sequence AC–II, greater subsidence occurred in the east, and uplift and erosion occurred in the center and west. The similar thickness in sequence AC–III across the three wells indicates a similar subsidence history.

A lithofacies cross section (Fig. 15) interprets the sequences in terms of the depositional model and correlations between the three wells. Deposition of the AC–I sequence began in the west in the Getty Lloyd Hurt well in deeper, intermittently oxygenated water on the outer ramp, after a rapid transgression over the Upper Eagle Ford sequence boundary. Sediment built up into shallower water and became fully oxygenated (inner ramp) in 'B–2' interval in this well. Deposition began in intermediate water depths (middle ramp) with enough oxygen to support horizontal burrowers in the Tesoro Valcher well on the San Marcos Arch. The 'C' and 'D' markers from the Getty Lloyd Hurt well are truncated by an unconformity in the Tesoro Valcher, based on a *Glossifungites* ichnofacies and glauconitic packstone at the equivalent level. A volcanic vent near the Valcher well erupted ash during the upper AC–I sequence. The area near the volcano was uplifted and was shallow enough that coarse-grained skeletal packstone could form over widespread thin ash. AC–I beds were tilted and truncated eastward in an angular unconformity during the middle to late Coniacian. In the Shefts Sallie Clark well east of the San Marcos Arch, composite sequence AC–I consists of 10 ft (3 m) of inner ramp facies, underlain by *Glossifungites* ichnofacies at the Austin Chalk–Eagle Ford contact and overlain by an 11 ft (3.4 m) glauconite bed. This area is interpreted to have experienced subaerial erosion due to periodic structural uplift, based on the very thin intervals in the basal Austin Chalk and underlying Eagle Ford Group, with 3 ft (1 m) Upper Eagle Ford, 9 ft (2.7 m) Lower Eagle Ford, and 5 ft (1.5 m) Pepper Shale.

Composite sequence AC–II consists of 58 ft (17.7 m) of inner ramp facies in the Getty Lloyd Hurt well. Sea level varied, based on multiple glauconitic lags with hardgrounds and lithoclasts in the 'B–1' interval in this well. This sequence is represented in the Tesoro Valcher well by a ~5 ft (1.5m) interval with glauconitic lag. Sequence AC–II begins in the Shefts Sallie Clark well with the 11 ft (3.4 m) glauconitic lag near the base of the Austin Chalk. The composite sequence is interpreted as deposited on the inner ramp, based on its updip location, the abundance of oyster banks, and the glauconitic lags in the upper part of the sequence. Sequence AC–II is truncated westward toward the San Marcos Arch and San Antonio, based on outcrop and subsurface correlations (Durham, 1957; Cooper et al., 2020). The AC–II sequence thickens downdip of Shefts Sally Clark into Giddings Field. The City Service Ivy and Prairie Marburger cores from this area have interbedded horizontally burrowed and laminated or layered sediment in this interval, that are interpreted as intermittently oxygenated outer ramp facies.

Upper Santonian–lower Campanian composite sequence AC–III is similar in all three wells. The sequence shows a rapid transgression at the base followed by regression and another transgression near the top. The upper part of the sequence is argillaceous, with well-developed, mainly horizontal burrows in the Getty Lloyd Hurt and Shefts Sallie Clark wells, indicating deeper water (outer ramp) at the transition into the shaly lower Anacacho/Sprinkle/Ozan formations. The Austin-Anacacho contact is a chalk-on-chalk contact in the Tesoro Valcher well, indicating a likely longer hiatus over the San Marcos Arch than on either flank.

Strike Cross Section

The Austin Chalk expands greatly to the west of the Getty Lloyd Hurt well and to the east of the Shefts Sallie Clark well (Fig. 16). Sequence boundaries were identified from the nannofossil biostratigraphy and glauconitic beds in the three key wells and other cores (Dravis, 1980; Loucks and Reed, 2022; Zheng et al., 2021). Correlations of the entire study area were based on the consistent log character of the glauconite-rich beds above sequence boundaries, and recognition of angular truncation below sequence boundaries.

New nannofossil biostratigraphy enables correlation of the different Austin Chalk nomenclature in the major petroleum fields on either side of the San Marcos Arch and the outcrop (Fig. 16). Different nomenclature is used to describe the Austin Chalk, because the subsurface markers are largely of different ages on either side of the arch. The very widespread 'C' and 'D' markers in Pearsall Field and across South Texas are eroded over the San Marcos Arch and farther east. The multiple markers in the middle Austin Chalk in Giddings Field and Central Texas are eroded over the San Marcos Arch and toward the west.

The stratigraphic ties from Pearsall Field to the outcrop are based on biostratigraphy in the Getty Lloyd Hurt and Tesoro Valcher wells, type sections in outcrop (Jiang, 1989), and updip correlations into San Antonio. Giddings Field is tied to the out-

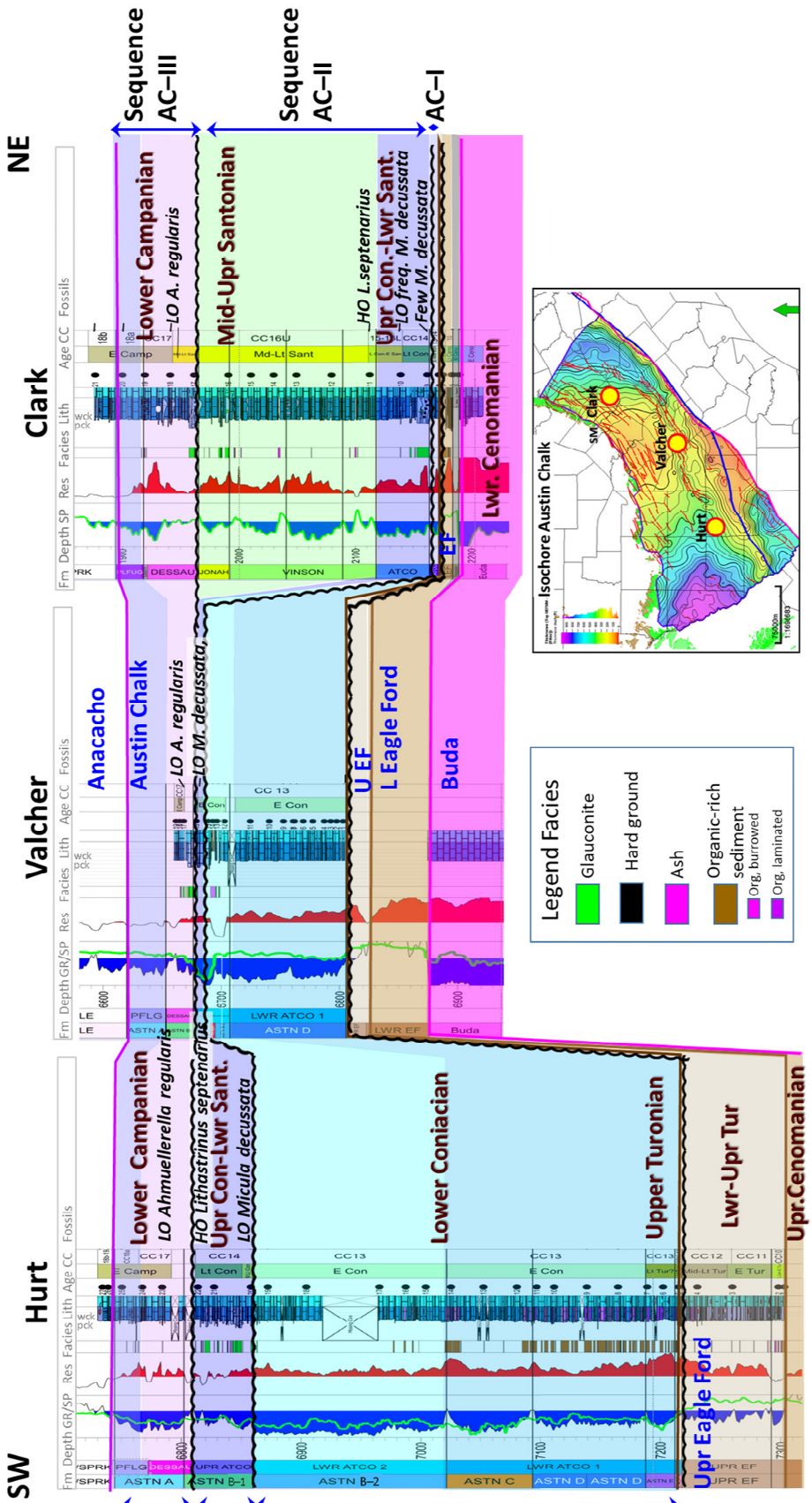

Figure 14. Biostratigraphic correlation of the three key wells, hung on the base of sequence AC–III (upper Santonian–Lower Campanian). Key fossils to note: lowest occurrence (LO) *Micula decussata* (middle Coniacian) at the base of sequence AC–II in dark blue; LO *Ahmuellerella regularis* (base lower Campanian) at the datum at the base of sequence AC–III in magenta; highest occurrence (HO) *Lithastrinus septenarius* (Lower Santonian) truncated under AC–III in the west (magenta over dark blue) and conformably overlain by middle-upper Santonian section in the east (green over dark blue). Note the co-occurrence of glauconitic lags (green in facies column) with biostratigraphic hiatuses. Nannofossils indicate dramatic asymmetry across the San Marcos Arch; the Lower Coniacian is very thick west of the arch, but almost absent east of the arch. Middle Santonian is thick east of the arch, but missing west of the arch.

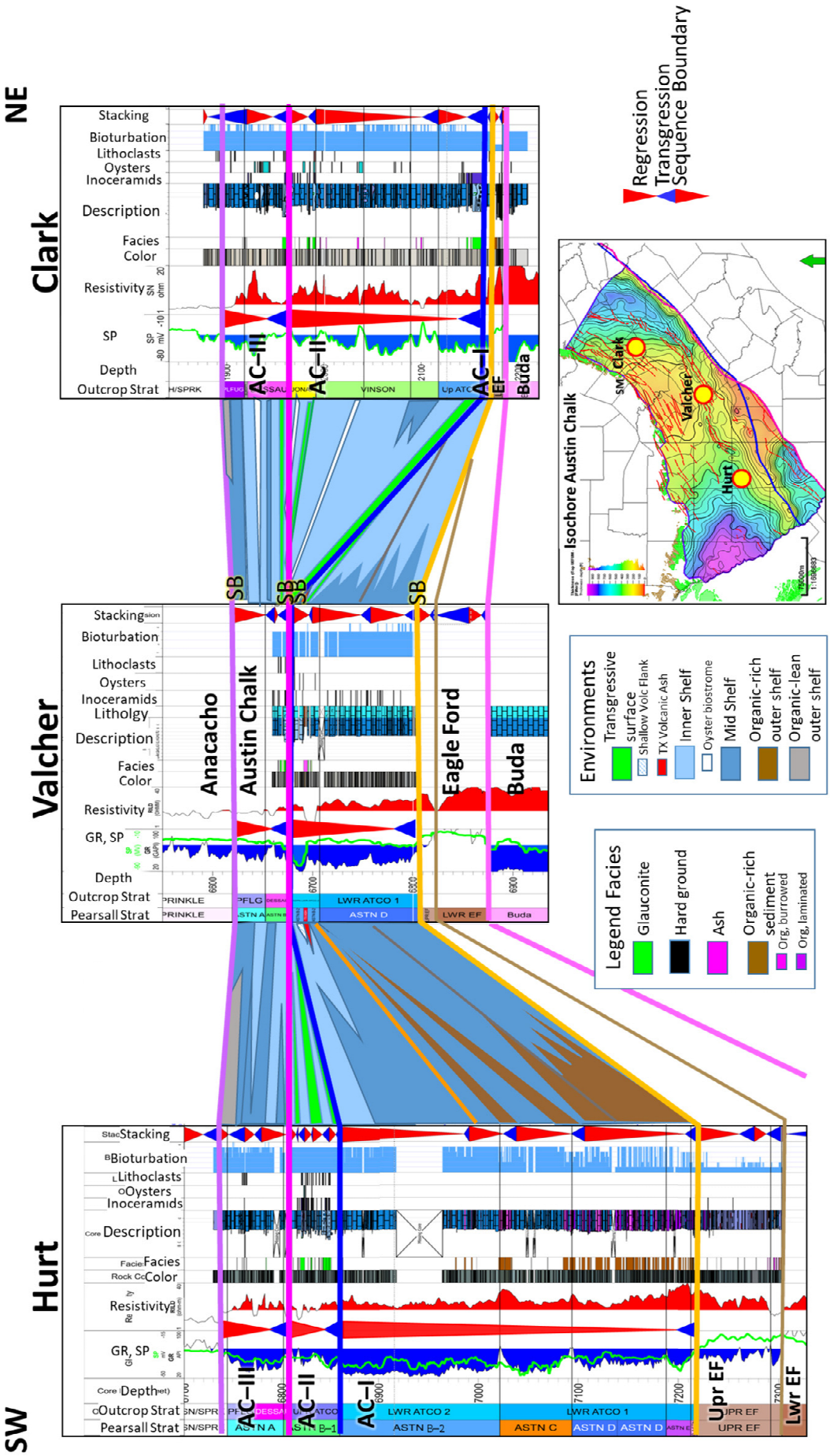

Figure 15. Austin Chalk lithofacies and sequences in the key three wells, hung on the base of sequence AC–III (upper Santonian–lower Campanian). Interpretation is based on nannofossil biostratigraphy and regional correlations. The Shefts Sallie Clark well, being farthest updip, is mostly inner ramp facies. The Tesoro Valcher well shows gradual shallowing in AC–I, absent AC–II, and inner to middle ramp facies in AC–III. The Getty Lloyd Hurt well shows gradual shallowing from outer to inner ramp in AC–I, inner ramp facies in AC–II, and middle to outer ramp facies in AC–III.

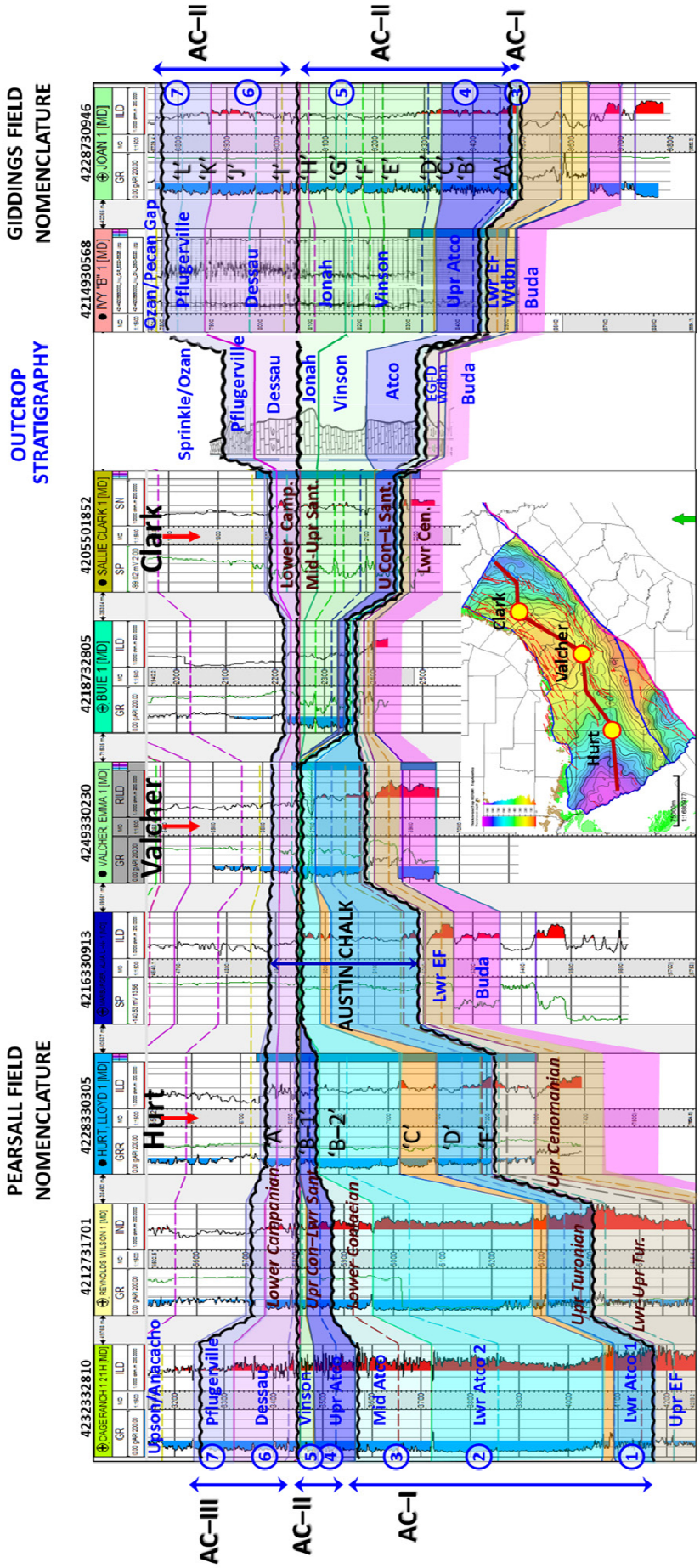

Figure 16. Well log strike cross section with correlation of the outcrop, Pearsall Field, and Giddings Field nomenclature, hung on the base of sequence AC–III (upper Santonian–Lower Campanian). The cross section shows the three composite sequences of the Austin Chalk and ties the nomenclature from the outcrop to nomenclature in the petroleum fields on either side of the San Marcos Arch, based on biostratigraphy, core, and log correlations. Outcrop nomenclature (Durham, 1957; Jiang, 1989; Young, 1985) is in blue. Letters 'A' through 'E,' west of the San Marcos Arch are from Pearsall Field nomenclature (Ewing, 2013), and letters 'A' through 'L,' east of the arch, are from Giddings Field nomenclature (Maranto, 2017). The blue circles numbered 1–7 define seven depositional sequences in the Austin Chalk. This cross section shows the major thickness changes in the sequences across the San Marcos Arch. Petroleum fields on either side of the arch have different stratigraphic nomenclature, because the major correlation markers are of different ages.

crop through nannofossil data at Shefts Sallie Clark and the outcrop (Jiang, 1989) and downdip correlations. Giddings 'A'–'C' correlate into the Atco Formation. The boundary between sequences AC–I and AC–II is within or at the top of the Giddings 'A' unit (Middle-Upper Atco). Composite sequence AC–II includes Giddings 'D'–'G' (Vinson Formation), and Giddings 'G'–'H' (Jonah Formation). Composite sequence AC–III includes 'H'–'K' I (Dessau Formation), and Giddings 'K'–'L' (Pflugerville Formation). The Burditt Formation was not tied between the outcrop and the subsurface. It is a thin, poorly exposed marl unit in outcrops in Austin, ~17 ft (~5.1 m) thick (Lundquist, 2015b), but it is not clearly recognizable in the subsurface.

A time-stratigraphic cross section (Wheeler diagram) (Fig. 17) was constructed for this strike line to show the stratigraphic continuities and hiatuses in the Austin Chalk, based on the reference nannofossil biostratigraphic chart (Fig. 10) and correlations indicating angular truncation. The three composite sequences in the Austin Chalk are separated by significant hiatuses. Composite sequence AC–I is subdivided into three higher order sequences (transgressive-regressive cycles), all equivalent to the Lower to Middle Atco Formation. Composite sequence AC–II is subdivided into two depositional sequences, the Upper Atco and the combined Vinson-Jonah formations. Composite sequence AC–III has two depositional sequences, the Dessau and the combined Burditt-Pflugerville formations. Sedimentation rates differ widely from east to west and from updip to downdip, in different sequences in the Austin Chalk.

It is remarkable how long the hiatuses are in this cross section, given that the main constituents of the Austin Chalk are pelagic nannofossils and microfossils, typically interpreted as deposited in a quiet water shelf setting. The angular truncation and thin intervals indicate that sedimentation was interrupted by long periods of submarine or subaerial erosion. The regional angular truncations are interpreted as formed due to regional tectonic movements rather than eustatic changes, which were relatively low magnitude during the Cretaceous (Sames et al., 2020) and would not have developed the asymmetry seen in this cross section.

Dip Cross Section

An oblique dip line (Fig. 18) extends from the well-documented Austin Chalk outcrop in San Antonio (Cooper et al., 2020), to the Getty Lloyd Hurt well (Loucks et al., 2020b), and across the relict Edward shelf edge (Ewing, 2013) onto the submarine plateau and the relict Sligo shelf edge. The Austin Chalk is thin in San Antonio, thickens into the Maverick Basin, and thins again near the relict Edwards shelf edge. The downdip thinning can be explained as due to: (1) structural movement (subsidence in the Maverick Basin and uplift at the relict shelf edge) or (2) sedimentary processes that formed depositional relief in the Austin Chalk (a depositional wedge or ramp thinning toward the Gulf of Mexico).

The depositional wedge or ramp model is favored for the Austin Chalk, based on the relative thicknesses of underlying and overlying formations and sediment architecture and facies within the Austin Chalk. The overlying Anacacho Formation thickens downdip as the Austin Chalk thins and continues to thicken beyond the relict Edwards shelf margin, as would be expected with greater subsidence and accommodation space toward the Gulf of Mexico. The high GR/high resistivity 'C' and 'D' correlation markers within the Austin Chalk show a sigmoidal offlapping geometry. They are thin and closely spaced updip, thicken in Pearsall Field, and thin and downlap onto the Eagle Ford Formation near the relict Edwards shelf edge to the south (Ewing, 2013). Facies at the base of the Austin Chalk, in the Well Y core in Karnes County, a few miles (several km) updip of the relict Edwards shelf edge, are dark colored and intermittently laminated and horizontally burrowed, indicating an intermittently oxygenated outer ramp setting. The vertical facies transition from poorly to fully oxygenated up section in the Getty Lloyd Hurt well also supports the idea of a depositional ramp, as it indicates shallowing water depths as the depositional ramp topography developed.

The depositional ramp interpretation postulates that the Maverick Basin was not a closed basin, but was open to the Gulf of Mexico during Austin Chalk deposition. The thickest Austin Chalk sediment was deposited in shallower water than the thinner sediment downdip at the relict shelf edge. Thicker updip sediment is likely associated with greater coccolith productivity, from increased nutrients and possible upwelling currents. Downdip thinning indicates non-deposition or erosion, due to less primary productivity or stronger bottom currents near the relict shelf edge. Later Upper Cretaceous sediments were unaffected by the relict shelf edge, as subsidence toward the Gulf of Mexico increased.

DISCUSSION

Ties to Existing Lithofacies Concepts

Cooper et al. (2020) recognized five proximal to distal facies in outcrops near San Antonio. Facies were placed along a subtidal ramp model, based on grain size and fossil content. Sequences in the Austin Chalk in San Antonio were defined by deepening- and shallowing-upward trends. Hardgrounds and firmgrounds indicate sequence boundaries, and glauconite-rich beds indicate transgressive surfaces. These were tied into the shallow subsurface to create a regional sequence stratigraphic framework. This study interprets the Austin Chalk as deposited on a similar ramp profile as Cooper et al. (2020), but extends the concepts downdip. Their outer ramp would be the middle ramp in this study. Hardgrounds and glauconite indicate sequence boundaries and transgressive tracts in both studies.

Five lithofacies were described in numerous cores from Austin Chalk wells in Texas and Louisiana (Loucks et al., 2020a; Loucks et al., 2020b; Loucks et al. 2021a; Loucks et al. 2021b). Facies were interpreted as deposited in a continuum from fully oxygenated to poorly oxygenated water. Oxygen levels were attributed to different water depths or different oceanic conditions. More abundant and diverse fossils in updip wells and in the upper Austin Chalk were interpreted as indicating less environmental stress or possibly shallower water (Loucks et al., 2020b, 2021b). All cored facies were interpreted as deposited below storm wave base based on the presence of coccoliths and planktonic foraminifera and the absence of hydrodynamic features. Further updip, the outcrop is interpreted to be nearer fair water wave base (Dravis, 1980; Loucks et al., 2020b) based on extensive *Thallasinoides*, oyster banks, and glauconite. Several different facies types in core are interpreted as debrites (Loucks and Reed, 2022), including poorly sorted glauconitic skeletal packstone with lithoclasts, coarse skeletal packstone and grainstone around volcanic tuff cones, and oyster concentrations. These facies were postulated to have formed by downslope gravity transport off volcanic highs or shallow water areas.

The lithofacies classification and interpretations in this study are similar to the classification and depositional models described above. The major difference is in postulating wider water depth variations during normal sedimentation and the presence of sequence boundaries and associated erosion and transgression. The presence of coccolithophores and planktonic foraminifera cannot rule out depositional environments shallower than storm wave base, because these organisms lived in the shallow water column and could have been passively transported into shallower water by surface currents. The absence of hydrodynamic features also is not definitive, as current features would have been unlikely to form in fine-grained chalk and would have been obliterated by

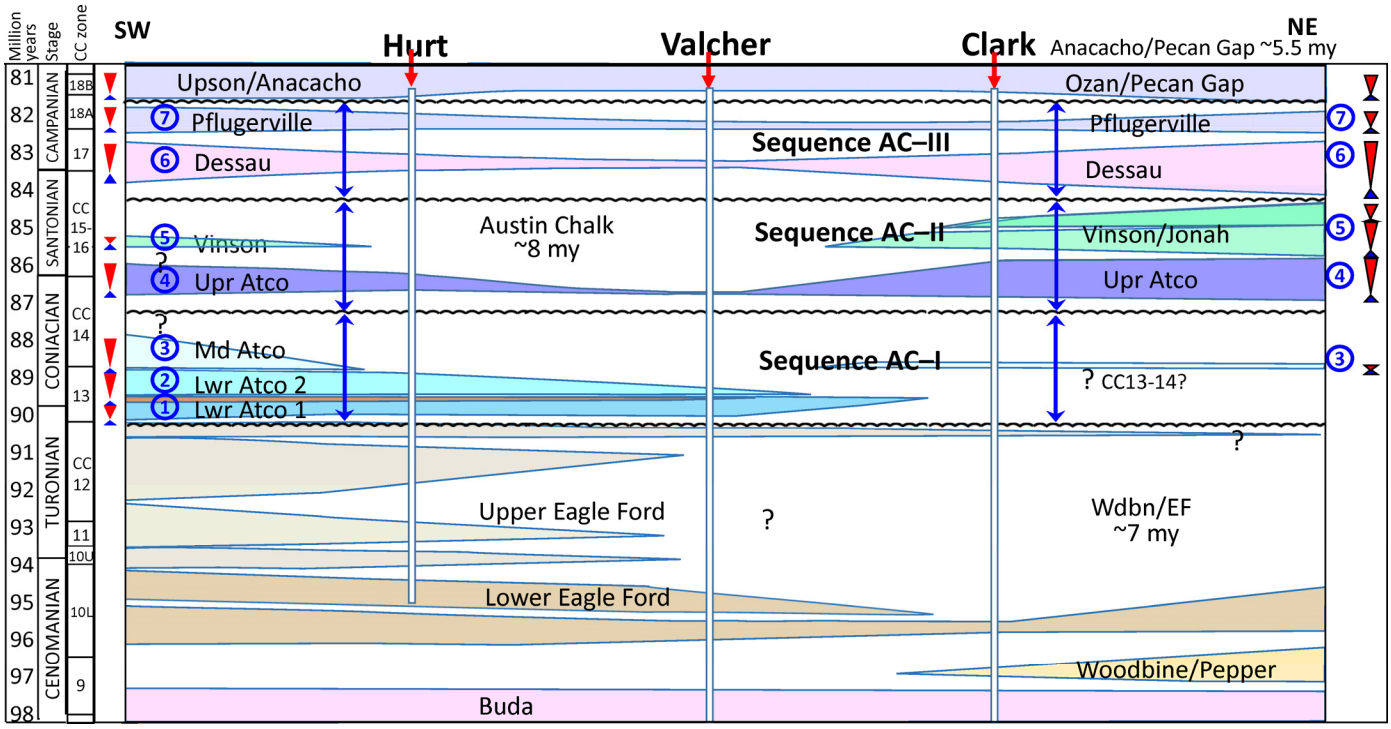

Figure 17. Strike cross section in time (Wheeler diagram). Time section shows large hiatuses during Eagle Ford and Austin Chalk deposition. The Austin Chalk unconformably overlies the Eagle Ford Group and is unconformably overlain by the Anacacho/Pecan Gap Formation. The Austin Chalk has three composite sequences (AC–I, AC–II, and AC–III), separated by late Coniacian and late Santonian unconformities. Seven depositional sequences, ~1 My in duration, are recognized (circles 1–7). The eastern area (the early San Marcos Arch) has hiatuses of several My separating very thin lower Austin and Eagle Ford formations (each only few feet thick). Uncertainty remains about placement of these thin sequences in time. The central area (the later San Marcos Arch) also has hiatuses of several My duration. The western area (subsiding Maverick Basin) has the least time missing. Composite sequence AC–I (depositional sequences 1–3) is thickest in the west but is truncated in the east. Sequence AC–II (depositional sequences 4–5) is thickest in the east, almost completely removed over the arch, and is thin in the west. A thin sequence AC–III (depositional sequences 6–7) extends across the San Marcos Arch but is thicker on the east side.

the extensive bioturbation. Evidence in the outcrop for water depths above storm wave base in the outcrop include: scours in Austin Chalk (e.g. Cooper et al., 2020; Dravis, 1980; Griffith et al., 2019; Hovorka, 1998; Young, 1985), hummocky cross beds in the unbioturbated D marker equivalent in Langtry (Griffith et al., 2019), ferruginous oolites near Eagle Ford Austin contact San Antonio (Cooper et al., 2020), and grainstone/packstone fragmental macrofossil concentrations in the Austin Chalk (e.g., Cooper et al., 2020; Durham, 1957; Young, 1985), and beach rock around Pilot Knob tuff cone (Young, 1985). These features occur across the outcrop belt, not just around San Antonio where water depths were shallowest, so similar conditions would be expected over large areas of the subsurface, especially over the San Marcos Arch.

One significant difference in interpretation between this study and other studies (Loucks et al., 2020b; Loucks and Reed, 2022) is the interpretation of the facies called 'debrites.' In this study, these facies are interpreted as formed in three different environments that are not primarily associated with down slope movement. Intervals with glauconitic and phosphatic skeletal packstone beds, with intraclasts and lithoclasts, are interpreted as transgressive lag deposits that overlie sequence boundaries, since they are associated with biostratigraphic hiatuses, have log character that can be traced widely across South and Central Texas, and overlie angularly truncated sections. The intraclasts and lithoclasts are interpreted as eroded firm grounds and hardgrounds. Glauconitic and phosphatic sediments were likely transported upslope as transgression advanced over a regional submarine or subaerial unconformity. The coarse-grained skeletal packstone and grainstone beds around local Texas volcanic tuff cones are interpreted to have formed nearly in place, in shallower water depths caused by local uplift during volcanism, given the small areal and vertical size of the tuff cones, and the wide extent of the coarse-grained carbonate facies. This facies migrated updip during later sea level rise. Oyster concentrations are interpreted to have formed in situ as extensive biostromes in updip settings, like those that enabled the stratigraphic correlation of the Austin Chalk in outcrop.

Application to Petroleum Geology of the Austin Chalk in Texas

Austin Chalk reservoir quality is controlled by the relative proportion of calcite vs. clay content, vertical heterogeneity, and thickness (Corbett et al., 1987, 1997; Martin et al., 2011; Rowe et al., 2017). The proportion of calcite controls the effective matrix porosity and mechanical strength or fracture potential. Argillaceous content impairs reservoir quality, whether distributed homogenously, as thin interlayers (horsetail stylolites), or as interbeds, since it fills the matrix porosity and impedes fracture growth. Vertical heterogeneity and relative thickness of chalk beds control selection of prospective areas and stratigraphic objectives.

The best reservoir zone in Pearsall Field, west of the San Marcos Arch, is the 'B–2' unit in the upper portion of the Austin Chalk (Ewing, 2013). Recent wells in South Texas target the westwardly expanding section between the 'B–1' and 'C' units, from areas updip and downdip of the relict Edwards shelf edge

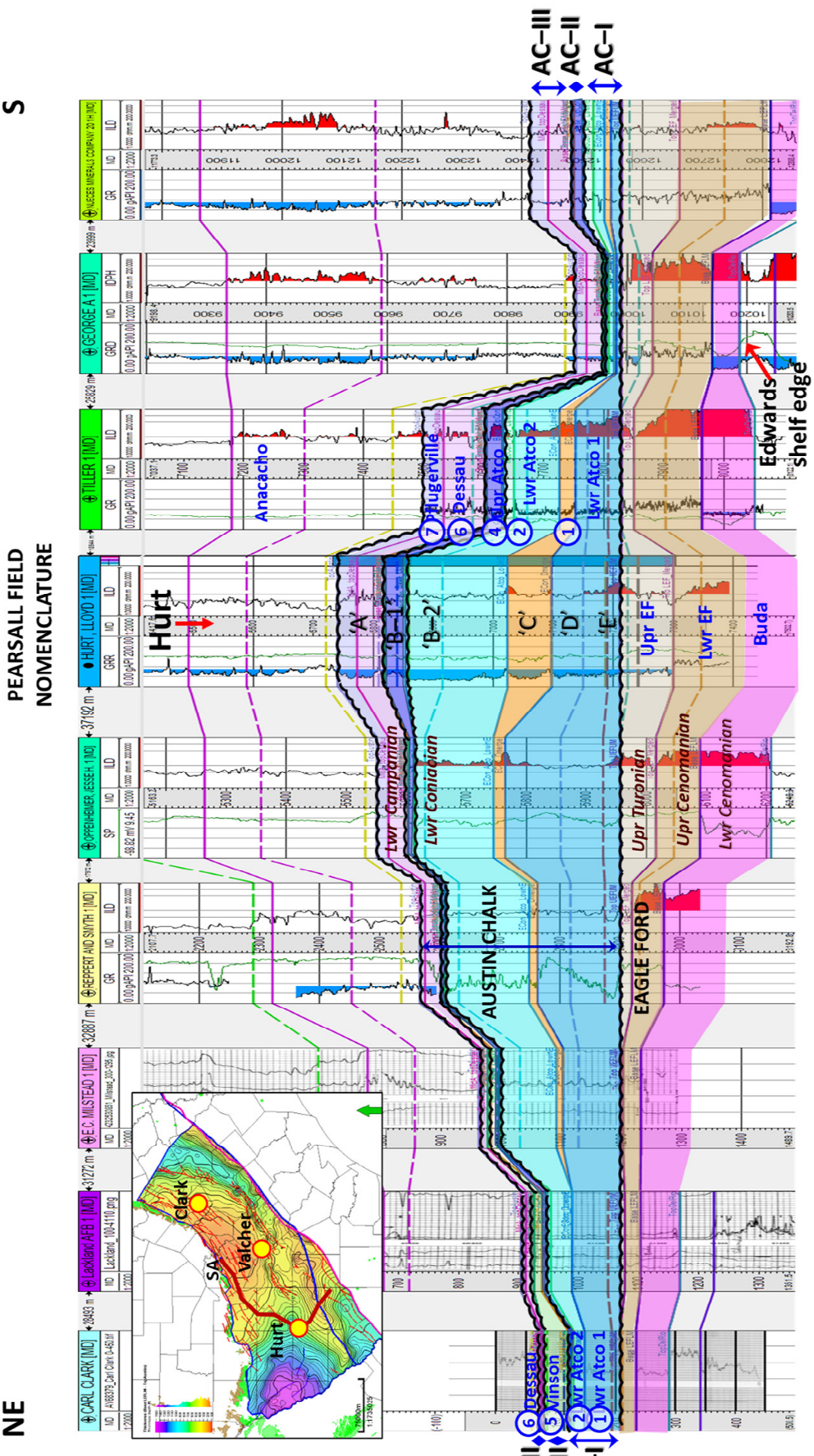

Figure 18. Oblique dip cross section from San Antonio outcrop and shallow subsurface (Cooper et. al., 2020) to Getty Lloyd Hurt well in Pearsall Field (Ewing, 2013; Loucks et. al., 2020b) to beyond the Edwards shelf edge. The Austin Chalk is interpreted as a depositional wedge or ramp, based on thickening of the overlying Anacacho interval, offlapping geometry of the organic-rich 'C' and 'D' units, and facies indicating shallower water upsection in the Getty Lloyd Hurt well and toward the outcrop belt in San Antonio.

(von Bassenheim and Taylor, 2023). The best reservoir zones in Giddings Field, east of the arch, are the 'A' and 'B' units near the base of the Austin Chalk (Maranto, 2017).

Based on nannofossil stratigraphy, the lower Coniacian 'B–2' reservoir (in sequence AC–1 of this study) in the upper Austin Chalk in Pearsall Field is older than the middle-upper Coniacian 'A' and 'B' reservoirs (upper AC–I, lower AC–II) near the base of the Austin Chalk in Giddings Field (Fig. 16). Younger Santonian and Campanian sections (in sequences AC–II and AC–III) in both fields are less productive, probably due to more admixed clay and more closely spaced bentonite and marl beds that inhibit fractures and upward migration.

A wide range of facies, from the inner to outer ramp, form productive reservoirs in the Austin Chalk. The coarse-grained skeletal packstone and grainstone units around the small Texas volcanoes (facies A) produce from structural-stratigraphic traps (Ewing, 1986) but only yield small volumes, due to their small areas, thicknesses, and porosity reduction during diagenesis. Inner ramp facies (facies B–D) in updip areas produce in structural-stratigraphic traps, and elsewhere are porous and wet. The Shefts Sallie Clark core, in Luling-Branyon Field, is an example of an updip reservoir having matrix porosity, where brown oil stained zones alternate with unstained zones. Luling-Branyon Field is a structural-stratigraphic trap that does not have a common oil water contact. Many wells were drilled into faults to intersect fractures, or within structural closure, and permeability was enhanced through acidizing and artificial fracturing (Doyle, 1955).

Austin Chalk reservoirs at Pearsall and Giddings Fields were deposited in different depositional settings. The Pearsall Field 'B–2' reservoir was deposited in an inner to middle ramp setting, based on light to medium gray bioturbated facies (facies D–E) in the Getty Lloyd Hurt core. Giddings Field 'A' and 'B' reservoirs were deposited in the middle to outer ramp, based on horizontally burrowed facies (facies E) interbedded with medium gray, organic-lean, finely layered facies (facies H) in the Cities Service Ivy and Prairie Marburger cores. These productive zones have little admixed clay or interbedded marl so they have rock properties favorable for fracture development and matrix porosity preservation.

In the recent downdip trend, operators target matrix porosity in areas that have few natural fractures (Darbonne, 2020; Maranto, 2017; Pickett, 2018). These areas can produce better than underlying Eagle Ford Group reservoirs or legacy Austin Chalk reservoirs. Some reservoirs produce from light to medium gray bioturbated facies (inner ramp facies D–E), like in Pearsall Field, whereas other produce from interbedded bioturbated and organic-rich laminated facies (mid-outer ramp facies E–G) in the middle or base of the chalk. In slope settings and on the submarine plateau, the medium gray, massive, but splintery (outer ramp facies I in well X) may be a good reservoir, due to mechanical properties that favor fracturing (as evidenced by splintery character).

Migration paths from mature organic-rich source rock into the Austin Chalk reservoirs also are important. The best Austin Chalk reservoirs occur in thick, clean, uniform chalk beds in the oil or gas window, or where faults and fractures allowed updip migration into non-mature areas. Although organic-rich intervals in the lower portion of the Austin Chalk in downdip settings contributed to hydrocarbon charge, the Eagle Ford Group is likely to be the main source for Austin Chalk production (Kornacki, 2018), since it is more extensive and is more organic-rich (Grabowski, 1995). Downdip Austin Chalk production is mainly gas, so reservoirs in this setting can be very productive, despite lower porosity and permeability.

CONCLUSIONS

Austin Chalk correlations are based on log character, tied to facies and sequence stratigraphic surfaces in core and outcrop. New nannofossil biostratigraphy is key to regional correlations, especially over the San Marcos Arch, where the Austin Chalk is thin, and log markers pinch out. Biostratigraphic hiatuses are collaborated by core observations, since hiatuses are associated with bored lithoclasts, *Glossifungites* ichnofacies, and coarse-grained glauconitic skeletal packstone lags. This facies is correlated over large distances and occurs above angularly truncated beds.

Austin Chalk depositional environments are recognized by their regional setting, large-scale geometries in cross sections, log character, and core observations of lithology, sedimentary structure, and biota. Austin Chalk facies range from fully aerobic inner ramp to anaerobic outer ramp settings. Inner ramp facies are light colored and include medium to coarse-grained skeletal packstone, oyster biostromes, and biotically diverse, burrowed, clean and argillaceous skeletal wackestone. Middle ramp environments are medium gray skeletal wackestone dominated by horizontal burrows. Outer ramp facies are medium to dark grey to brown interbedded laminated organic-rich and horizontally burrowed skeletal wackestone, indicating intermittent anaerobic conditions.

The Austin Chalk is comprised of three composite sequences (AC–I, AC–II, and AC–III), bounded by a basal and upper unconformity and two internal unconformities, one in the upper Coniacian and a second in the upper Santonian. Considerable time is missing at hiatuses. Composite sequences begin with a rapid transgression, followed by deeper water facies, which gradually shallow below a sequence boundary, if the sequence is not erosionally truncated. Chalk distribution is extremely asymmetric across the San Marcos Arch. The lower Coniacian section is very thick west of the arch but is almost completely eroded on the east side. The Santonian section is very thick east of the arch but is eroded in the center and on the west side of the arch. Thickness trends in the Lower Campanian section are similar to the Santonian section. The Austin Chalk thins dramatically to the south near the relict Lower Cretaceous Edwards margin in South Texas. The chalk forms a wedge of sediment, a depositional ramp that thins at the downdip edge due to slower sedimentation and more active bottom currents.

New nannofossil biostratigraphy in this study enables a tie to the Cretaceous stages and between the outcrop lithostratigraphy and different stratigraphic nomenclature in the petroleum fields on either side of the San Marcos Arch. Similar lithofacies distinctions are made by all investigators of the Austin Chalk, but sequence stratigraphic interpretations in this study involve a greater range of water depths and fluctuations in relative sea level. Most of the variation in relative sea level is attributed to tectonic movement rather than eustatic changes. The most productive petroleum reservoirs in the Austin Chalk are in the lower Coniacian west of the San Marcos Arch and in the upper Coniacian east of the arch. Reservoirs occur in multiple depositional environments, from the inner to outer ramp. Productive reservoir limits are controlled by reservoir thickness, argillaceous content, vertical heterogeneity of beds, burial depth, and access to charge.

ACKNOWLEDGMENTS

I would like to acknowledge Texas A&M University students, Eric Peavey and Roy Conte for help in the field, Molly McCreary and Samantha MacKenzie for core XRF, and John Sarao for nannofossil biostratigraphic analyses in several cores and outcrops. I would like to thank John Cooper and Alexis Godet at the University of Texas San Antonio sharing the biostratigraphic analysis of the Tesoro Valcher and their knowledge about the San Antonio outcrop. I appreciate conversations with many other geologists about correlations in the Upper Cretaceous. I am grateful for access to well log data from Enverus DrillingInfo, S&P Global–IHS Markit, and MJ Logs; cores from industry, USGS, and BEG; and software from Schlumberger Petrel and EasyCore. I appreciate the financial support for out-

crop and core work from AAPG, GCAGS, and the TAMU Berg-Hughes Center.

REFERENCES CITED

Ahr, W., 1973, The carbonate ramp: an alternative to the shelf model: Gulf Coast Association Geological Societies Transactions, v. 23, p. 221–225.

Alshuaibi, A. A., 2006, Coniacian to lowermost Campanian stratigraphy of the Austin Chalk, northeast Texas: Ph.D. Thesis, University of Texas at Dallas, 220 p.

Bralower, T. J., and J. A. Bergen, 1998, Cenomanian-Santonian calcareous nannofossil biostratigraphy of a transect of cores drilled across the Western Interior Seaway, *in* W. E. Dean and M. A. Arthur, eds., Stratigraphy and paleoenvironments of the Cretaceous Western Interior Seaway: Society of Economic Paleontologists and Mineralogists Concepts in Sedimentology and Paleontology 6, p. 59–77, <https://doi.org/10.2110/csp.98.06.0059>.

Bergen, J., and P. Sikora, 1999, Microfossil diachronism in southern Norwegian North Sea chalks: Valhall and Hod fields: Geological Society, London, Special Publications, v. 152, p. 85–111, <https://doi.org/10.1144/gsl.sp.1999.152.01.06>.

Blakey, R. C., 2013, NAM_key85Ma_LateK, Niobrara seaway, Late Cretaceous (Santonian) 85 Ma (87–83), North American key time slices, <https://deeptimemaps.com/>.

Buatois, L. A., and M. G. Mángano, 2011, Ichnology: Organism-substrate interactions in space and time, Cambridge University Press, 371 p. <https://doi.org/10.1017/cbo9780511975622>.

Cobban, W. A., S. C. Hook, and K. McKinney, 2008, Upper Cretaceous molluscan record along a transect from Virden, New Mexico, to Del Rio, Texas: New Mexico Geology, v. 30, p. 75–92.

Cohen, K. M., D. A. T. Harper, P. L. Gibbard, and N. Car, 2022, International chronostratigraphic chart: International Commission on Stratigraphy, <https://stratigraphy.org/ICSchart/ChronostratChart2022-02.pdf>.

Conte, R. A., 2020, Chronostratigraphic and geochemical characterization of the Cenomanian-Turonian Eagle Ford Group in West and South Texas, USA: Ph.D. Dissertation, Texas A&M University, 205 p.

Cooper, J. R., A. Godet, and M. C. Pope, 2020, Tectonic and eustatic impact on depositional features in the Upper Cretaceous Austin Chalk Group of south-central Texas, USA: Sedimentary Geology, v. 401, p. 1–17, <https://doi.org/10.1016/j.sedgeo.2020.105632>.

Corbett, K., M. Friedman, and J. Spang, 1987, Fracture development and mechanical stratigraphy of Austin Chalk, Texas: American Association of Petroleum Geologists Bulletin, v. 71, p. 17–28, <https://doi.org/10.1306/94886d35-1704-11d7-8645000102c1865d>.

Corbett, K., D. Van Alstine, and J. Edman, 1997, Stratigraphic controls on fracture distribution in the Austin Chalk: an example from the First Shot Field, Gonzales Co., Texas: American Association of Petroleum Geologists Hedberg Conference, Reservoir scale deformation—Characterization and prediction, June 22–28, 1997, p. 1–6.

Corbett, M., D. Watkins, and J. Pospichal, 2014, A quantitative analysis of calcareous nannofossil bioevents of the Late Cretaceous (late Cenomanian–Coniacian) Western Interior Seaway and their reliability in established zonation schemes: Marine Micropaleontology, v. 109, p. 30–45, <https://doi.org/10.1016/j.marmicro.2014.04.002>.

Darbonne, N., 2020, East Texas Chalk: It's the matrix: Hart Energy, Oil and Gas Investor, <https://www.hartenergy.com/exclusives/east-texas-chalk-its-matrix-184985>.

Dawson, W., B. Katz, and V. Robison, 1995, Austin Chalk (!) petroleum system Upper Cretaceous, southeastern Texas: A case study: Gulf Coast Association of Geological Societies Transactions, v. 45, p. 157–163.

Denne, R., and J. Breyer, 2016, Part 2: Regional depositional episodes of the Cenomanian–Turonian Eagle Ford and Woodbine Groups of Texas, *in* J. A. Breyer, ed., The Eagle Ford Shale: A renaissance in US oil production: American Association of Petroleum Geologists Memoir 110, p. 87–133, <https://doi.org/10.1306/13541959m1103660>.

Denne, R. A., J. A. Breyer, T. H. Kosanke, J. M. Spaw, A. D. Callender, R. E. Hinote, M. Kariminia, N. Tur, Z. Kita, and J. A. Lees, 2016, Part 1: Biostratigraphic and geochemical constraints on the stratigraphy and depositional environments of the Eagle Ford and Woodbine Groups of Texas, *in* J. A. Breyer, ed., The Eagle Ford Shale: A renaissance in US oil production: American Association of Petroleum Geologists Memoir 110, p. 1–86, <https://doi.org/10.1306/13541957m1103660>.

Diegel, F. A., J. Karlo, D. Schuster, R. Shoup, and P. Tauvers, 1995, Cenozoic structural evolution and tectono-stratigraphic framework of the northern Gulf Coast continental margin, *in* M. P. A. Jackson, D. G. Roberts, and S. Snelson, eds., Salt tectonics: A global perspective: American Association Petroleum Geologists Memoir 65, p. 109–151. <https://doi.org/10.1306/m65604c6>.

Doyle, W. M., 1955, Production and Reservoir Characteristics of the Austin Chalk in South Texas: Gulf Coast Association Geological Societies Transactions, v. 5, p. 3–10.

Dravis, J. J., 1980, Sedimentology and diagenesis of the Upper Cretaceous Austin Chalk formation, South Texas and northern Mexico: Ph.D. Thesis, Rice University, 513 p.

Dravis, J. J., 1991, Regional depositional setting and porosity evolution of the Austin Chalk Formation, South Texas, *in* S. Chuber, ed., Austin Chalk exploration symposium: Geology, geophysics and formation evaluation: South Texas Geological Society Special Publication, p. 17–23.

Dravis, J. J., 2018, Influence of reactivated basement faults on the porosity evolution of South Texas Cretaceous carbonates—Implications for Austin Chalk play development in Texas and Louisianan: South Texas Geological Society Bulletin, October 2018 issue.

Durham, C. O., 1957, The Austin Group in Central Texas: Ph.D. Thesis, Columbia University, 54 p.

Durham, C. O., and S. B. Hall, 1991, The Austin Chalk—Bed by bed through Central Texas, *in* S. Chuber, ed., Austin Chalk exploration symposium: Geology, geophysics and formation evaluation: South Texas Geological Society Special Publication, p. 25–40.

Enverus, 2022, Drillinginfo, <https://www.enverus.com/>.

Ewing, T. E., 1986, Balcones volcanoes in South Texas: Exploration methods and examples, *in* W. L. Stapp, L. A. Dutton, B. R. Weise, L. P. Jones, and W. G Fergeson, eds., Contributions to the geology of South Texas, 1986: South Texas Geological Society Special Publication, p. 368–379.

Ewing, T., R. Budnik, J. Ames, D. Ridner, and R. Dillon, 1990, Tectonic map of Texas: Bureau of Economic Geology, scale 1:750,000.

Ewing, T. E., 2003, Review of the tectonic history of the lower Rio Grande border region, South Texas and Mexico, and implications for hydrocarbon exploration, *in* N. C. Rosen, ed., Structure and stratigraphy of South Texas and northeast Mexico: Applications to exploration: Gulf Coast Section Society Economic Paleontologists and Mineralogists Foundation and South Texas Geological Society, p. 7–21.

Ewing, T. E., 2004, A nonspecialist's guide to the volcanology and petrology of the Balcones Igneous Province, *in* T. E. Ewing, ed., Volcanoes, asphalt, tectonics and groundwater in the Uvalde area, southwest: South Texas Geological Society Guidebook 2004–1: San Antonio, Texas, Gulf Coast Association of Geological Societies, p. 24–34.

Ewing, T. E., 2011, Tectonic domains in the Rio Grande Rio Bravo border region, Texas and Mexico: Laramide structures suggest earlier history: Gulf Coast Association of Geological Societies Transactions, v. 61, p. 141–155.

Ewing, T. E., 2013, Stratigraphy of the Austin, Eagle Ford, and Anacacho formations and its influence on hydrocarbon resources, Pearsall Field area, South Texas: Gulf Coast Association of Geological Societies Transactions, v. 63, p. 213–225.

Ewing, T. E., 2016, Texas through time; Long Star geology, landscapes, and resources: Bureau of Economic Geology, 431 p.

Ewing, T. E., 2018, The peripheral graben system in Texas: An overview: Gulf Coast Association Geological Societies Transactions, v. 68, p. 163–178.

Ferrill, D. A., M. A. Evans, R. N. McGinnis, A. P. Morris, K. J. Smart, D. Lehrmann, K. D. Gulliver, and Z. Sickmann, 2020, Fault zone processes and fluid history in Austin Chalk, southwest Texas: American Association of Petroleum Geologists Bulletin, v. 104, p. 245–283, <https://doi.org/10.1306/04241918168>.

Fiduk, J. C., L. E. Anderson, and M. G. Rowan, 2009, The structural control of South Texas Upper Wilcox shelf margin and slope facies deposition by extensional rafting: Salt tectonic and petroleum exploration implications: South Texas Geological Society Bulletin, v. 49, no. 7, p. 13–36.

Gale, A., P. Montgomery, W. Kennedy, J. Hancock, J. Burnett, and J. McArthur, 1995, Definition and global correlation of the Santonian-Campanian boundary: *Terra Nova*, v. 7, p. 611–622, <https://doi.org/10.1111/j.1365-3121.1995.tb00710.x>.

Gale, A. S., W. J. Kennedy, J. A. Lees, M. R. Petrizzo, and I. Walaszczyk, 2007, An integrated study (inoceramid bivalves, ammonites, calcareous nannofossils, planktonic foraminifera, stable carbon isotopes) of the Ten Mile Creek section, Lancaster, Dallas County, North Texas, a candidate Global Boundary Stratotype Section and Point for the base of the Santonian Stage: *Acta Geologica Polonica*, v. 57, p. 113–160.

Gale, A. S., J. M. Hancock, W. J. Kennedy, M. R. Petrizzo, J. A. Lees, I. Walaszczyk, and D. S. Wray, 2008, An integrated study (geochemistry, stable oxygen and carbon isotopes, nannofossils, planktonic foraminifera, inoceramid bivalves, ammonites and crinoids) of the Waxahachie Dam Spillway section, North Texas: a possible boundary stratotype for the base of the Campanian Stage: Cretaceous Research, v. 29, p. 131–167, <https://doi.org/10.1016/j.cretres.2007.04.006>.

Gale, A., J. Mutterlose, S. Batenburg, F. Gradstein, F. P. Agterberg, J. Ogg, and M. R. Petrizzo, 2020, The Cretaceous Period, in F. M. Gradstein, J. Ogg, M. D. Schmidt, and G. Ogg, eds., Geologic time scale 2020, v. 2, Elsevier, p. 1023–1086, <https://doi.org/10.1016/b978-0-12-824360-2.00027-9>.

GEOINFOMEX, 2019, Servicio Geológico Mexicano—GEOINFOMEX, <https://www.sgm.gob.mx/GeoInfoMexGobMx/>.

Goldhammer, R., and C. Johnson, 2001, Middle Jurassic–Upper Cretaceous paleogeographic evolution and sequence-stratigraphic framework of the northwest Gulf of Mexico rim, *in* C. Bartolini, R. T. Buffler, and A. Cantu-Chapa, eds : The western Gulf of Mexico Basin: Tectonics, sedimentary basins, and petroleum systems: American Association of Petroleum Geologists Memoir 75, p. 45–81, <https://doi.org/10.1306/m75768c3>.

Grabowski, G. J., 1981, Origin, distribution and alteration of organic matter and generation and migration of hydrocarbons in Austin Chalk, Upper Cretaceous, southeastern Texas: Ph.D. Thesis, Rice University, 276 p.

Grabowski, G. J., 1995, Organic-rich chalks and calcareous mudstones of the Upper Cretaceous Austin Chalk and Eagleford formation, south-central Texas, USA, *in* B. J. Katz, ed., Petroleum source rocks: Springer-Verlag, p. 209–234, <https://doi.org/10.1007/978-3-642-78911-3_12>.

Griffith, C., M. Pope, K. Gillespie, A. Godet, and D. Minisini, 2019, Facies in the Lower Austin Chalk Group, from a roadcut on US 90 and a core behind the outcrop, near Langtry, Texas: GeoGulf Transactions, v. 69, p. 79–95.

Griffith, C. M., 2023, Regional sequence stratigraphy, biostratigraphy, facies, and depositional environments of the Upper Cretaceous Austin Chalk in South and Central Texas: Ph.D. Dissertation, Texas A&M University, 259 p.

Hancock, J. M., and I. Walaszczyk, 2004, Mid-Turonian to Coniacian changes of sea level around Dallas, Texas: Cretaceous Research, v. 25, p. 459–471, <https://doi.org/10.1016/j.cretres.2004.03.003>.

Haq, B. U., J. Hardenbol, and P. R. Vail, 1987, Chronology of fluctuating sea levels since the Triassic: Science, v. 235, p. 1156–1167, <https://doi.org/10.1126/science.235.4793.1156>.

Hayes, J. M., 2021, Austin Chalk stratigraphy, Giddings Field to the San Marcos Arch, Central Texas: M.S. Thesis, Texas A&M University.

Hendrix, C. K., 2016, Chemolithofacies of the Upper Cretaceous Buda Formation and Austin Chalk Group, south-central Texas: a product of integration of lithologic and chemical data: M.S. Thesis, University of Texas, 127 p.

Holifield, R., 1982, Austin Chalk trend Upper Gulf Coast, Texas—Keynote address, Austin Chalk oil recovery conference at Texas A&M University, April 28, 1982: Texas Petroleum Research Committee Bulletin 256, p. 1–27.

Hovorka, S., 1998, Facies and diagenesis of the Austin Chalk and controls on fracture intensity—A case study from north-central Texas: University of Texas at Austin: Bureau of Economic Geology Geological Circular 2, 47 p., <https://doi.org/10.23867/gc9802d>.

Jiang, M., 1989, Biostratigraphy and geochronology of the Eagle Ford Shale, Austin Chalk, and lower Taylor Marl in Texas based on calcareous nannofossils: Ph.D. Dissertation, Texas A&M University, 575 p.

Juárez-Arriaga, E., T. F. Lawton, Y. Z. E. Ocampo-Díaz, D. F. Stockli, and L. Solari, 2019, Sediment provenance, sediment-dispersal systems, and major arc-magmatic events recorded in the Mexican foreland basin, north-central and northeastern Mexico: International Geology Review, v. 61, p. 2118–2142, <https://doi.org/10.1080/00206814.2019.1581848>.

Koger, C., 1981, Depositional and diagenetic history of the Austin Chalk, Central Texas, and its relationship to petroleum potential: M.S. Thesis, Baylor University, 151 p.

Kornacki, A. S., 2018, Production of migrated oil from horizontal wells landed in the Eagle Ford Formation on the San Marcos Arch: Unconventional Resources Technology Conference Paper URTEC–2871569–MS, 17 p., <https://doi.org/10.15530/urtec-2018-2871569>.

Lee, C.–T. A., H. Jiang, E. Ronay, D. Minisini, J. Stiles, and M. Neal, 2018, Volcanic ash as a driver of enhanced organic carbon burial in the Cretaceous: Scientific Reports, v. 8, Paper 4197, 9 p., <https://doi.org/10.1038/s41598-018-22576-3>.

Loucks, R., J. Lambert, K. Patty, T. Larson, R. M. Reed, and C. Zahm, 2020a, Regional overview and significance of the mineralogy of the Upper Cretaceous Austin Chalk Group, onshore Gulf of Mexico: Gulf Coast Association Geological Societies Journal, v. 9, p. 1–16.

Loucks, R. G., T. E. Larson, C. Y. Zheng, C. K. Zahm, L. T. Ko, J. E. Sivil, P. Sheng, S. C. Ruppel, and W. A. Ambrose, 2020b, Geologic characterization of the type cored section for the Upper Cretaceous Austin Chalk Group in southern Texas; A combination fractured and unconventional reservoir: American Association of Petroleum Geologists Bulletin, v. 104, p. 2209–2245, <https://doi.org/10.1306/04222019197>.

Loucks, R. G., R. M. Reed, L. T. Ko, C. K. Zahm, and T. E. Larson, 2021a, Micropetrographic characterization of a siliciclastic-rich chalk; Upper Cretaceous Austin Chalk Group along the onshore northern Gulf of Mexico, USA: Sedimentary Geology, v. 412, Paper 105821, p. 1–19, <https://doi.org/10.1016/j.sedgeo.2020.105821>.

Loucks, R. G., C. Zahm, T. Larson, L. Zahm, and P. Zeng, 2021b, Stratal architecture, lithofacies, environmental setting, depositional processes, and associated geological characteristics of the Upper Cretaceous Austin Chalk in Louisiana: Gulf Coast Association Geological Societies Journal, v. 10, p. 47–75.

Loucks, R. G., and R. M. Reed, 2022, Implications for carbonate mass-wasting complexes induced by volcanism from Upper cretaceous Austin Chalk strata in the Maverick Basin and San Marcos Arch areas of south-central Texas, USA: Sedimentary Geology, v. 432, Paper 106120, p. 1–18, <https://doi.org/10.1016/j.sedgeo.2022.106120>.

Lowery, C. M., 2013, Foraminiferal biostratigraphy and paleoecology of the Turonian-Coniacian Austin Chalk in West Texas: Geological Society of America Abstracts with Programs, v. 45, no. 7, p. 332.

Lundquist, J. J., 2001, Foraminiferal biostratigraphic and paleoceanographic analysis of the Eagle Ford, Austin, and lower Taylor

Groups (middle Cenomanian through lower Campanian) of Central Texas: Ph.D. Thesis, University of Texas at Austin, 566 p.

Lundquist, J. J., 2015a, The Austin Chalk Group in Travis County, Texas - An introduction to Upper Cretaceous paleogeography, depositional episodes, and large-scale stratigraphic framework of the northeastern Gulf of Mexico, *in* C. P. D. Sullivan, ed., Austin Chalk (UK)—Stratigraphic, geophysical, hydrogeological and hydrocarbon exploration/production characteristics: Austin Geological Society Guidebook 36, p. 1–16.

Lundquist, J. J., 2015b, The Austin Chalk Group in Travis County, Texas: Review of lithostratigraphic and biofacies characteristics, significant field exposures, and the construction of a composite stratigraphic section, *in* C. P. D. Sullivan, ed., Austin Chalk (UK)—Stratigraphic, geophysical, hydrogeological and hydrocarbon exploration/production characteristics: Austin Geological Society Guidebook 36, p. 39–82.

Male, F., and C. Zahm, 2021, Regional productivity in the Austin Chalk with emphasis on fault zone production in the Karnes Trough area, Texas: GeoGulf Transactions, v. 71, p. 173–183.

Maranto, A., 2017, The Austin Chalk revival: Society of Petroleum Engineers Gulf Coast Section Business Development Group, 25 p., <https://www.spegcs.org/media/files/files/7afb8c32/Austin_Chalk_Maranto_8fPCS8Z.pdf>.

Martin, R., J. D. Baihly, R. Malpani, G. J. Lindsay, and W. K. Atwood, 2011, Understanding production from Eagle Ford–Austin Chalk system: Society of Petroleum Engineers Paper SPE–145117MS, 28 p.

Matthews, T., 1986, The petroleum potential of "serpentine plugs" and associated rocks Central and South Texas: Baylor Geological Studies Bulletin, v. 44, p. 1–43.

McCreary, M. E., 2022, Chemostratigraphic and sequence stratigraphic analysis of the Austin Group in the outcrops and subsurface of Texas: M.S. Thesis, Texas A&M University, 36 p.

Minisini, D., J. Eldrett, S. C. Bergman, and R. Forkner, 2018, Chronostratigraphic framework and depositional environments in the organic-rich, mudstone-dominated Eagle Ford Group, Texas, USA: Sedimentology, v. 65, p. 1520–1557, <https://doi.org/10.1111/sed.12437>.

Ogg, J., and L. Hinnov, 2012, Chapter 27: Cretaceous, *in* F. M. Gradstein, J. G. Ogg, M. Schmitz, and G. Ogg, eds., The geologic time scale 2012: Elsevier, p. 793–853, <https://doi.org/10.1016/b978-0-444-59425-9.00027-5>.

Ogg, J. G., G. Ogg, and F. M. Gradstein, 2016, Cretaceous, A concise geologic time scale: 2016: Elsevier, p. 167–186, <https://doi.org/10.1016/b978-0-444-59467-9.00013-3>.

Pearson, K., 2012, Geologic models and evaluation of undiscovered conventional and continuous oil and gas resources: Upper Cretaceous Austin Chalk: U.S. Geological Survey Scientific Investigations Report 2012–5159, 26 p., <https://doi.org/10.3133/sir20125159>.

Perch-Nielsen, K., 1985, Mesozoic calcareous nannofossils, *in* H. M. Bolli, J. B. Saunders, and K. Perch-Nielsen, eds., Plankton stratigraphy: Cambridge University Press, p. 329–426, <https://doi.org/10.1002/gj.3350250216>.

Pessagno, E. A., 1969, Upper Cretaceous stratigraphy of the western Gulf Coast area of Mexico, Texas, and Arkansas: Geological Society of America Memoir 111, 139 p., <https://doi.org/10.1130/mem111-p1>.

Phelps, R. M., C. Kerans, R. G. Loucks, R. O. Da Gama, J. Jeremiah, and D. Hull, 2014, Oceanographic and eustatic control of carbonate platform evolution and sequence stratigraphy on the Cretaceous (Valanginian–Campanian) passive margin, northern Gulf of Mexico: Sedimentology, v. 61, p. 461–496, <https://doi.org/10.1111/sed.12062>.

Pickett, A., 2018, The Eagle Ford and Austin Chalk better operating practices and new approaches keep South Texas humming: The American Oil and Gas Reporter, <https://www.aogr.com/magazine/sneak-peek-preview/and-new-approaches-keep-south-texas-humming>.

Roy, E. C., M. Eidelbach, and N. Trumbly, 1981, A Late Cretaceous calcarenite beach complex associated with submarine volcanism, Wilson County, Texas: Gulf Coast Association Geological Societies Transactions, v. 31, p. 173–178.

Rowe, H., E. Sivil, C. Hendrix, S. Narasimhan, A. Benson, A. Morrell, G. Torrez, and P. Mainali, 2017, Defining linkages between chemofacies and mechanical stratigraphy in the Austin Chalk: Implications for geomechanics and induced fracture simulations: Unconventional Resources Technology Conference Paper URTEC–2668845–MS, p. 572–579, <https://doi.org/10.15530/urtec-2017-2668845>.

Sames, B., M. Wagreich, C. P. Conrad, and S. Iqbal, 2020, Aquifer-eustasy as the main driver of short-term sea-level fluctuations during Cretaceous hothouse climate phases: Geological Society of London Special Publications, v. 498, p. 9–38, <http://doi10.1144/sp498-2019-105>.

Short, D., 2018, Tectonics of the Texas portion of the Sabine Island: Gulf Coast Association of Geological Societies Transactions, v. 68, p. 493–516.

Sissingh, W., 1977, Biostratigraphy of Cretaceous calcareous nannoplankton: Netherlands Journal of Geosciences/*Geologie en Mijnbouw*, v. 56, p. 37–65.

Stephenson, L. W., 1937, Stratigraphic relations of the Austin, Taylor, and equivalent formations in Texas: U.S. Geological Survey Professional Paper 186–G, p. 133–146, <https://doi.org/10.3133/pp186g>.

Taff, J. A., 1892, Reports of the Cretaceous are north of the Colorado River, I, The Bosque division, II, The Lampasas-Williamson section: Third Annual Report of the Geological Survey of Texas, p. 269–373.

Texas Railroad Commission, 2022, Historical Production, Eagle Ford Shale, 2008 to current, <https://www.rrc.texas.gov/oil-and-gas/major-oil-and-gas-formations/eagle-ford-shale/>.

Texas Water Science Center (USGS TWSC), 2014, Geologic database of Texas: Geologic maps compiled by the Bureau of Economic Geology, digitized by US Geological Survey with cooperation of the Texas Natural Resources Information System, <https://data.tnris.org/collection?c=79a18636-3419-4e22-92a3-d40c92eced14#4.8/31.32/-100.08>.

Thompson, M. E., 1986, Stratigraphy of the Dale Lime and its relation to structure at Bateman Field, Bastrop County, Texas, *in* W. L. Stapp, L. A. Dutton, B. R. Weise, L. P. Jones, and W. G. Fergeson, eds., Contributions to the geology of South Texas: South Texas Geological Society, p. 356–367.

Thompson, M. E., 2019, A revised age range for Texas Gulf Coast serpentine mounds: South Texas Geological Society Bulletin, v. 59, no. 5, p. 19–33.

von Bassenheim, D., and P. Taylor, 2023, Webb County chalkstars: Geologic drivers and activity trends: GeoGulf Transactions, v. 72, p. 481.

Young, K., D. Grunig, M. A. Jordan, D. L. Parker, and E. Jones, 1977, Guidebook to the geology of the Travis County: University of Texas Geological Society, 170 p.

Young, K., 1985, The Austin division of Central Texas, *in* K. Young, and C. Woodruff, eds., Austin chalk in its type area—Stratigraphy and structure: Austin Geological Society Guidebook 7, p. 3–51.

Young, K., 1986, Cretaceous, marine inundations of the San Marcos Platform, Texas: Cretaceous Research, v. 7, p. 117–140, <https://doi.org/10.1016/0195-6671(86)90013-3>.

Zahm, C., 2020, Improved mechanical and natural fracture model of the Lower Austin Chalk using outcrop, core, and well logs, Central Texas: Gulf Coast Association Geological Societies Transactions, v. 70, p. 361–371.

Zheng, C. Y. C., R. G. Loucks, C. Kerans, and L. T.–W. Ko, 2021, Benthic oxygenation history of South Texas during the Austin Chalk Group deposition: An integrated ichnologic, sedimentological, and geochemical study: American Association of Petroleum Geologists/Society of Exploration Geophysics International Meeting for Applied Geoscience and Energy convention.

Zheng, C. Y. C., C. Kerans, L. A. Buatois, M. G. Mángano, and T. Ko, in press, Sedimentary environment and benthic oxygenation history of the Austin Chalk Group, South Texas: An integrated ichnologic, sedimentologic, and geochemical approach: Sedimentology.